Front. Chem. Sci. Eng. 2025, 19(11): 103
https://doi.org/10.1007/s11705-025-2606-6

REVIEW ARTICLE

Advancement in membrane spacer technology: emerging trend and modification of three-dimensional printed membrane spacers for fouling mitigation

Nili Mastura Munir[1], Ebrahim Mahmoudi (✉)[1], Siew Fen Chua[1], Nur Ameera Rosli[1], Alireza Nouri[1], Mohsen Mesbahi Babaei[2], Amir Mohammad Najafi[3], Hasan Nikkhah[4], Ng law Yong[5], Ang Wei Lun[1], Abdul Wahab Mohammad[6]

1 Department of Chemical and Process Engineering, Faculty of Engineering and Built Environment, Universiti Kebangsaan Malaysia, Bangi 43600, Malaysia
2 School of Chemical, Petroleum and Gas Engineering, Iran University of Science and Technology (IUST), Tehran 16846–13114, Iran
3 Department of Chemical and Petroleum Engineering, Sharif University of Technology, Tehran 14588–89694, Iran
4 Department of Chemical and Biomolecular Engineering, University of Connecticut, Storrs 06269, USA
5 Lee Kong Chian Faculty of Engineering and Science, Universiti Tunku Abdul Rahman, Jalan Sungai Long, Bandar Sungai Long, 4300 Kajang, Selangor 43000, Malaysia
6 Chemical and Water Desalination Engineering Program, College of Engineering, University of Sharjah, Sharjah 27272, United Arab Emirates

Abstract Aside from being essential for human needs, water resources are also in demand by various industries to ensure the sustainability of economic development in countries. However, the supply of clean and affordable water is slowly depleting to the point where it becomes a major issue that requires significant attention. The membrane filtration system is an effective method for purifying water, with a high potential to provide clean water with minimal energy. The membrane spacer is a significant component in the membrane filtration system that considerably influences its performance. The dominant challenge in membrane spacers is fouling, mainly biofouling, which leads to unwanted consequences that drastically decrease the system's performance. This review focuses on the advancements in membrane spacer technology through the modification of geometric design, selection of materials, and evaluation of their impact on fluid dynamics and biofouling. Additionally, the review provides insight into the utilization of three-dimensional printing methods and three-dimensional simulations in advancing membrane spacer technology.

Keywords membrane spacer, fouling, geometric design, material, 3D printing

1 Introduction

Sustainable resources are being extensively studied due to the demand from the increasing human population and expanding economic infrastructure. Continuous exploration and the provision of resources at reduced costs are increasingly essential to ensure the well-being and security of the global community. Water is one of the primary resources required by every industry, contributing to the ever-growing need for more research focusing on affordable and accessible supply and usage [1,2].

The availability of water resources has been facing a significant challenge since the rate of water consumption is double the rate of population growth [3]. The United Nations (UN) reports that two-thirds of the global population could face strained situations, with the possibility of inhabiting areas with no water available to most people [4]. In addition to the increase in global population, other factors contribute to future water shortage issues, such as rapid urban growth, rural poverty, and an increase in human migration [1]. Additionally, the presence of micropollutants such as pesticides, pharmaceuticals, inorganic molecules, and other aromatic organic compounds flowing into water bodies, mainly in industrialized and developing countries, increases the demand for purified water. Membrane separation processes are rapidly developing for water and wastewater treatment due to their significant role in water

Received April 23, 2025; accepted July 18, 2025; online September 1, 2025

E-mail: mahmoudi.ebi@ukm.edu.my

purification [5].

Membrane technology has been implemented in various industries due to its high selectivity, minimal chemical utilization, possible industrial scale-up, and lower energy requirements [6−10]. Aside from water treatment industries, other sectors depend heavily on membrane technology, including electrodialysis, energy, food, and pharmaceutical industries [11]. The general processes involved in membrane technology include pressure-driven membrane processes, electrochemical charge-driven processes, and emerging membrane processes [12,13]. It is crucial to enhance the overall performance of the membrane by avoiding performance drops in membrane separation systems [14].

The feed spacer, whether mesh spacers, channel spacers, or feed channels, is an essential component that creates feed channels between membrane leaves by placing the spacer on top of the membrane filtration to allow water to pass over the membrane surface [15]. Additionally, the spacer can assist in foulant removal by generating turbulence over the feedwater flow, creating a shear force between the surface of the membrane and the spacer. This process increases flow mixing, enhances mass transfer, and decreases the concentration polarization (CP) phenomenon [14,16,17].

However, the presence of the feed spacer can cause two major problems: resistance due to the feed channel pressure (FCP) and the presence of stagnant zones that appear between the membrane and feed spacer, as well as at the intersection of spacer filaments. FCP can lead to increased energy loss, which occurs when the feed spacer resists fluid flow and worsens when fouling occurs [18]. The stagnant zone, on the other hand, reduces flow and increases the deposition of foulants, exacerbating CP phenomena and fouling, ultimately raising water production costs [13,19].

The irreversible fouling on membrane and feed spacer surfaces caused by numerous organic, inorganic, and biological substances has been a significant issue for membrane technology processes that may reduce membrane performance [19]. Feed spacers are typically not designed to withstand high-pressure flow and are costly to replace. Thus, selecting an optimum feed spacer design according to the application is highly important to ensure the compatibility of the feed spacer with the process operation [14,19].

Membrane spacer design geometry, such as the filament diameter, shape and pattern, mesh length, and spacer thickness, has significant impacts on the feed channel hydrodynamics, fouling, and other process parameters [20]. The advancement of feed spacer geometry design is facilitated by the rise of three-dimensional (3D) printing technology, which allows for custom and complex designs using different materials [6,21,22]. Geometry design, materials, and 3D printing have been proven to improve the feed spacer in terms of fouling and biofouling resistance in addition to membrane materials or membrane properties. Suitable feed spacers compatible with the filtration process can increase the efficiency of the filtration system, thus lowering energy consumption. However, there are limited studies that focus on the feed spacer in detail. This study evaluates the advancement of the feed spacer through modifications to its geometric design, materials, and the 3D printing method used for spacer fabrication, aiming to increase membrane filtration efficiency and reduce the fouling tendency of the feed spacer. This review focuses specifically on pressure-driven membrane processes, including ultrafiltration (UF), reverse osmosis (RO), and nanofiltration (NF), where spacers in the feed chamber play a critical role in mitigating fouling and enhancing mass transfer. In addition, this study also evaluates recent studies on two-dimensional (2D) and 3D simulation, numerical modeling of the feed spacer, and future perspectives for membrane spacer technology.

1.1 Significance of this review

Membrane technology is a topic that has been discussed extensively to date, encompassing various branches such as water purification, desalination, electrolysis, and gas separation. Owing to the influence of membrane spacers on the efficiency and lifespan of a membrane system, research and studies focusing on membrane spacers have begun to grow alongside the continuously increasing discussion focusing on membrane technology. According to Lin et al. [13], the publications of membrane spacers can be categorized into three phases: phase one (hydrodynamics), two (biofouling mitigation), and three (3D printing technology). Phase one includes the publications from the year 2001 until 2008, where the research mainly focused on the parameters of hydrodynamics or hydraulic performances such as mass transfer and pressure drop of the system that utilizes feed spacer. No published literary works before 2009 have experimented with the alteration of feed spacers to mitigate biofouling. Phase two, which started in 2009 and continued until 2015, initially began when Lin et al. [13] reported in their research that feed spacers largely contributed to biofouling phenomena. This finding has encouraged feed spacer fields to move toward biofouling mitigation rather than hydraulic performance considerably. Phase three began shortly after phase two, where additive manufacturing (AM) via 3D printing enhanced the studies of spacers with novel designs. These novelly designed spacers are intended to improve both hydraulic and biofouling prevention of membrane systems. As of late, the center of discussion in the field of membrane spacer has been associated with various scopes, such as 3D printing in membrane spacer technology [23], fouling mitigation [24], biofouling [25], and modification of membrane spacer [26].

Novel ideas and research continue to arise as there is still a wide gap of unknown possibilities in this field. The publishing trend discussing membrane spacers in the past 10 years is shown in Fig. 1. This finding was conducted by retrieving publication information from Scopus with the keywords 'membrane' and 'spacer' for the past 10 years. The number of publications in the membrane spacer field is considerably lower than that in membrane technology; however, the trend has steadily increased over the years. Based on the growing trend, it is clear that the membrane spacer field is gaining continuous interest from researchers and will emerge more over the years. However, there is still limited extensive discussion regarding the relationship between membrane technology and membrane spacers, the effect of membrane spacer modification toward fouling, and the advancement of the membrane spacer field through 3D printing. This review serves the purpose of filling in these gaps, where the advancement of membrane spacers is discussed thoroughly to aid further research focusing on this field.

2 Membrane fouling

2.1 Membrane fouling: types, factors, and mechanisms

Membrane fouling can influence the likelihood of membrane spacer fouling. In general, membrane fouling often refers to the deposition or adsorption of dissolved or suspended particles onto the membrane pores or surfaces. Membrane fouling negatively impacts membrane performance through various interactions. Pore blockages, pore constrictions, and cake formations are typically responsible for membrane fouling [27]. Different interactions between the membrane and the feed solution lead to various types of fouling [28]. These can be categorized based on the characteristics of the foulant, including inorganic and scaling fouling, colloidal and particulate fouling, organic fouling, and biological fouling. Figure 2 shows the types of fouling and the factors causing them.

Fig. 1 Growing trend of publications in membrane spacer.

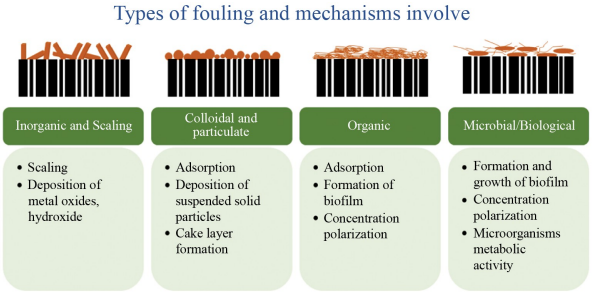

Fig. 2 Types of fouling and mechanisms involved.

2.1.1 Inorganic and scaling fouling

Inorganic fouling occurs when inorganic substances or precipitates, such as metal oxides, metal hydroxides, and minerals, accumulate on the membrane surface or within the membrane pores [29]. Scaling is among the typical examples of inorganic fouling, which is caused by the deposition of supersaturated dissolved minerals on the membrane. Substances commonly found in membrane influents that could cause membrane inorganic fouling or scaling include $BaSO_4$, $CaCO_3$, $CaSO_4$, SiO_2, and many other inorganic compounds [30,31].

During a membrane filtration process, as the feed solution with dissolved minerals permeates through the membrane, the inorganic substances are retained on the membrane surface. The concentration of dissolved minerals on the membrane surface increases and eventually exceeds the solubility limit. Supersaturation of the dissolved minerals on the membrane surface induces the aggregation of dissolved minerals to form a cluster of inorganic solid particles via nucleation. The formed nuclei can further attract the deposition of more mineral molecules, leading to crystallization, and larger clusters of crystals will form as the aggregation of minerals continues [32]. These scaling crystals then interact with the membrane surface via electrostatic attraction or adsorption. Lastly, a scaling layer builds up on the membrane surface, causing undesired membrane fouling.

2.1.2 Colloidal and particulate fouling

Colloidal and particulate fouling are associated with the accumulation of solid particles on the membrane surface [33]. Colloidal particles are relatively smaller, usually ranging from nanometers to micrometers, whereas particulate fouling involves particles ranging from micrometers to millimeters in size. The presence of non-biological organic matter (natural organic matter (NOM) and proteins) and inorganic particles (silt and silica) usually leads to this type of fouling [34].

These suspended particles in the membrane filtration influent can be attracted to the membrane surface via van der Waals forces and electrostatic interactions. As the

filtration and deposition of the colloidal particles on the membrane surface continue, the membrane pores may become blocked, forming cake layers on the membrane surface [35]. The cake layer can accelerate the fouling rate by trapping and attracting additional particles, reducing the membrane's overall performance.

2.1.3 Organic fouling

Organic fouling is a type of fouling caused by the attachment of organic substances to the membrane surface. The feed water or wastewater influent may include various types of organic matter, such as NOM, a combination of fulvic acids and humic acid, and additional NOM resulting from the decomposition of animal and plant waste [36]. The organic compounds are usually large and can easily cause physical blockages of membrane pores. Additionally, organic substances can actively interact with membrane surfaces through adsorption [37].

The organic foulants can easily adhere to and accumulate on the membrane, forming a cake layer. As filtration continues, the concentration of organic substances retained on the membrane surfaces increases, creating a CP layer on the membrane surface [38]. This layer further encourages the adsorption and deposition of more organic molecules. As a result, the hydraulic resistance of the membrane increases, leading to a decline in membrane flux. In addition, CP also promotes the formation of a biofilm that leads to biological fouling.

2.1.4 Biological fouling

Biological fouling, or biofouling, is a condition where a biofilm is formed due to the growth and accumulation of microorganisms. Biofouling contributes to more than 45% of membrane fouling, among other types of membrane fouling. Extracellular polymeric substances (EPS) are usually produced by microorganisms (e.g., algae, bacteria, fungi, and others) as one of their survival tactics and shelter [39]. EPS in the biofilm consists of organic polymers made up of extracellular DNA, lipids, proteins, and polysaccharides. It forms a matrix in which all the microorganism communities are embedded.

The issue with biofouling on the membrane spacer dates back to 1994, when Flemming et al. [40] stated that biofilm could completely overgrow the membrane spacer and prevent its hydraulic function. An observation was made in the late 1900s by Baker et al. [41] that the deposition of fouling occurs first along the spacer filaments before it disperses onto the membrane surface. A few years later, van Paassen et al. [42] observed a relationship between biofouling on feed spacers and the increase in FCP drop in the system. There has been much research conducted to improve the geometry design of membrane spacers up until recently, which stems from the suggestion by Ridgway in 1997, who proposed the theory of optimizing the spacer design to enhance hydrodynamics and aid with biofouling mitigation [43]. Even though studies regarding biofouling focus more on membrane improvements today, there is an increased trend in the study of membrane spacers as the primary fundamental aspect of biofouling phenomena [44]. This is supported by a study by Vrouwenvelder et al. (2009) [47,48], where the biofouling of feed spacers has been shown to have a more significant impact on FCP drop compared to other aspects such as membrane type, transmembrane pressure, and permeate flux. Fluid dynamics, the study of fluid flow and the associated forces, is commonly described by vector equations such as the Navier-Stokes equations, and is an important factor in the field of membrane spacer technology [45]. Thus, many studies are conducted to study the fluid dynamics of the membrane spacer, mainly using computational fluid dynamics (CFD). CFD is the numerical simulation of these fluid flows, where the governing equations are solved to predict how fluids behave under various conditions [46]. Their study on 3D CFD modeling also discovered that dead zones caused by membrane spacers that obstructed the flow increased biofouling [47,48].

The removal of biofilm can be categorized into three mechanisms: desorption, detachment, and dispersal. The desorption mechanism works in reverse, as bacterial attachment does, such as when surface-attached cells dissociate from the substratum following the flow of the bulk liquid. Detachment mechanisms refer to the process of the passive dislocation of biofilm-embedded cells from the biofilm due to the alteration of biofilm structure that is caused by external forces. Biofilm dispersion refers to the spreading of biofilm-embedded cells from the biofilm when there are environmental changes. Although this mechanism typically occurs to enhance the spreading of biofilm on the surface, its inducers can bring harm to the biofilm as well [49]. Due to the high reproductive capability of microorganisms, those attached to the membrane will grow in the membrane matrix over time, with or without pre-treatment for microbial cell removal. The growth of microorganisms is supported by the biodegradable materials present in the membrane feed [50,51].

Consequently, the biofilm will thicken and form a complex layer, inducing CP. Additionally, these microorganisms will produce by-products such as organic acids, extracellular enzymes, and other large compounds through metabolic activities. These by-products will further encourage the growth of a thicker biofilm. The biofilm will also trigger organic fouling as it provides an additional matrix layer for the adhesion of organic particles. Hence, biofouling poses a significant challenge for membrane filtration, especially in water and wastewater treatment.

2.2 Membrane fouling challenges and the hydrodynamic role of spacers

Fouling usually leads to unwanted outcomes that significantly deteriorate membrane performance. First, the cake layer or biofilm generated on the membrane surface reduces membrane flux during fouling [52]. The deposition of solid particles within the membrane pores or on the membrane surface has been found to restrict water transportation, reducing membrane permeability. Hence, a higher operating pressure would be needed to maintain the desired system flow rate and output volume, resulting in higher energy consumption and operational costs.

Besides, fouling could compromise membrane selectivity. In inorganic fouling, scaling could alter the membrane pore size through membrane blockage, significantly affecting the membrane's rejection ability. In the case of biofouling, when microorganisms attach to the membrane surface, other unwanted particles could pass through the membrane during the filtration process, reducing membrane separation performance. Besides, fouling could also increase the chances of membrane damage, and increase the frequency of membrane cleaning and maintenance [53,54]. Thus, fouling mitigation has always been one of the top priorities and research interests in membrane technology.

Many fouling mitigation methods have been researched and employed, and improvements are still being made. One of the conventional mitigation methods is pretreatment, which can be employed to reduce fouling by pre-screening the feed solution to prevent large colloid particles from entering the membrane filtration stage [55]. Technologies like adsorption, coagulation-flocculation, and pH adjustment can also be applied before membrane filtration [28,56]. Chemical additives like antiscalants, dispersants, and biocides can be added to the feed solution to reduce the chances of fouling and foulant attachment [57,58]. Most types of fouling can be controlled to a great extent by various pre-treatment methods. However, biofouling remains a significant challenge even after extensive water pre-treatment [59].

In addition to pretreatment, membrane modification has also been one of the research interests. Antifouling property is generally defined as a surface or material's ability to resist or prevent the accumulation of undesired biological or particulate matter, such as microorganisms, organic compounds, or other fouling agents [60]. Implementing or enhancing antifouling properties by the addition of nanoparticles with antibacterial properties is one of the common methods used in many studies. Different nanoparticles could be incorporated during membrane modification to prepare membranes with antifouling properties and enhanced filtration performance. Nanoparticles like silver, carbon, and graphene-based nanomaterials are usually suggested for the preparation of membranes with antibacterial and antifouling properties [61−63]. Adding a suitable membrane feed spacer is considered one of the most promising methods to mitigate membrane fouling. The feed spacer plays a vital role in eliminating potential foulants by placing it on top of the membrane during a filtration process to induce turbulence over the feedwater flow and generate shear force between the membrane surface and the spacer [64]. In addition to acting as a support for the membrane, the feed spacer can provide additional water paths and promote flow in the filtration channels.

Lin et al. [65] studied the dynamic evolution and spatial distribution of biomass in feed spacer channels to signify the effect of membrane spacer clearance in the development of biofouling. In this study, four feed spacers with different filament diameters (0.4, 0.45, 0.55, and 0.6 mm) were used, which formed four feed spacers with different channel porosities (0.882, 0.851, 0.777, and 0.735). A 20 d of long-term biofouling test was conducted, and a feed solution with low nutrient concentration was used to imitate practical conditions. During this test, the changes in FCP drop and biofouling distribution were observed. It is reported that the initial stage of biofouling formation on the membrane is mainly influenced by the shear stress effects. The feed spacer with the lowest porosity (highest filament diameter) had high average wall shear stress, which led to relatively low membrane biofouling. Meanwhile, the feed spacer with the highest porosity (lowest filament diameter) exhibited a high tendency for biofilm to form at the region with low wall shear stress, such as the contact area between the feed spacer and the membrane surface and the central area of the spacer meshes. During the middle and late stages, the continuous accumulation of biomass caused a "blocking effect", and it intensified more in the low-porosity feed channel. Biofilm is prone to build up in the clearance of the spacer, which hinders the flow passage and lowers the uniformity of the flow field. This blockage leads to a significant increase in FCP drop and an expansion of the "dead zone" area, which worsens the rate of membrane biofouling. Based on this report, it is suggested that modifying the feed spacer channel to improve hydrodynamics does not avoid biofouling entirely; rather, it reduces the rate of biofouling on the membrane and reduces energy consumption.

2.2.1 Turbulence flow

The direct deposition of scaling compounds such as $BaSO_4$ and $CaCO_3$ can be prevented by enhancing the turbulent flow of the membrane. A study was conducted by Løge et al. [66], which concluded that the impact of crystallization fouling attachment and detachment processes is surface- and flow-dependent. It is explained that in a turbulent flow condition, the influx of ionic

materials increases, which shortens the diffusion period from the feed water to the surface. Additionally, the residence time of materials decreases sharply, which is caused by the higher flow rate. This causes a minimal time for the fluid to react on a cell surface. Promoting turbulent flow in a membrane system will effectively lower the time for the foulant to accumulate, as they are being swept away before they can accumulate on the membrane surface. Furthermore, the short residency time of the fluid in the membrane channel significantly reduces the possibility for the foulant to adhere to the membrane surface. This phenomenon will ensure the prevention of nucleation and crystal growth and, ultimately, scaling on the membrane surface.

Enhancement of flow turbulence in the membrane system can be achieved with the employment of a membrane spacer, which will also increase the average velocity, shear rate, and water flux, and decrease the flux decay rate [67]. Turbulent conditions are promoted through the presence of the spacer's filaments, which act as baffles in the flow stream [68]. The intensity of a spacer's turbulence highly depends on the geometry of the spacer, such as the number of filament layers, mesh length, the diameter of the filament, and the orientation angle of the mesh. Aside from the geometry, the cross-flow velocity and Reynolds number for the filtration system also have a high impact on the intensity of the spacer's turbulence. When the velocity drop increases in the flow field, the turbulence intensity of the spacer increases [69].

2.2.2 Shear stress

One of the significant hydrodynamic factors that can be manipulated to mitigate membrane fouling, mainly in wastewater treatment, is shear stress. The concentration boundary layer may be disrupted through shear stress, which will lead to an increase in the mass transfer coefficient at the interface between the membrane and solution, thus leading to a decrease in CP [70]. A study by Awais et al. [71] showed that a strong shear force across a surface causes the elimination of deposits. Furthermore, since shear stress has the ability to generate lift force, increasing the shear stress will increase the number of particles that are swept away from the membrane surface due to the dominant back-transport mechanisms [72]. This is supported by a study conducted by Wray et al. [73], which proved that the back-transport of soluble materials in natural water ecosystems, including biopolymers that increase membrane fouling, can be encouraged through shear stress. There are various methods to create shear stress in a membrane system, including rotation, membrane spacer, varied gas bubble, fluid dynamic gauging, turbulence promoter, and vibration. As of now, membrane spacers are the most common method to promote shear stress and mass transfer in spiral-wound flat sheet NF and RO elements [74].

Even though the hydrodynamic factors caused by membrane spacers, such as turbulent flow and shear stress, reduce fouling of the membranes, other factors, such as the characteristics of the membrane spacers also play a vital role in mitigating fouling. The study to optimize the design of the spacer stems from its potential to control the fluid flow on the membrane surface, which determines the performance of the filtration, fouling mitigation, and CP [75]; hence, it has become a major study topic in the membrane field. There are many studies that investigate the flow dynamics that are caused by a membrane spacer's geometric design to improve fouling mitigation, such as altering the fiber cross-sections of the membrane spacers [76−78]. The material used for fabricating the spacer also contributes greatly to the performance of the membrane system [79]. The diverse porosity properties of the materials used offer many advantages in increasing the efficiency of the system, mainly materials with regulated pore size distributions or porous polymers [80]. With the emergence of 3D printing technology, numerous materials have been experimented with, such as acrylonitrile butadiene styrene (ABS), polycaprolactone, polypropylene (PP), and polylactic acid (PLA), for the fabrication of spacers [81].

Thus, this study aims to shed light on membrane feed spacer technology aimed at overcoming membrane fouling issues. The details on issues arising from traditional membrane feed spacers and the advancement of membrane feed spacers through different fabrication and modification methods will be thoroughly evaluated in the following sections.

3 Modification of feed spacer

3.1 Geometric design of spacer

Flow distribution, turbulence promotion, shear stress distribution, and pressure drop are factors that will be highly impacted by the design of the spacer. Designing the geometry of the spacer properly helps to ensure a uniform flow distribution across the membrane surface, ensuring that the entire membrane area is utilized efficiently. This can prevent the formation of stagnant or uneven flow areas. In addition to that, an efficient geometry can increase turbulence in the flow channels, leading to increased mass transfer and reduced formation of boundary layers. The turbulence helps to minimize CP and fouling on the membrane spacer, thereby increasing the performance of the filtration system. The distribution of shear stress on the membrane spacer is also affected by the spacer geometry. A controlled and uniform shear stress can help to reduce fouling by minimizing the

particles or foulants deposited on the membrane surface.

When designing the membrane spacer, the frictional resistances caused by the design need to be taken into consideration. A spacer design with high frictional resistance can increase the pressure drop, which can lower the overall performance of the filtration system. Nonetheless, the geometric design of the spacer is still an ongoing research project aimed at fabricating an optimum design for the spacer to enhance membrane filtration.

One of the types of spacers commercially produced today is the net spacer. This type of spacer has two basic configurations: nonwoven and woven. The nonwoven configurations, consisting of two layers of straight filaments, represent the most basic form, while the woven configurations can be divided into partially woven and fully woven, as shown in Fig. 3 [82]. For each spacer configuration, the efficiency in controlling fouling is determined by the geometric parameters of the spacer, which include spacer thickness, filament diameter, internal strand angle, mesh size, and spacer orientation (shape and pattern) [83]. Figure 4 illustrates a spacer with dimensions of length (L), width (W), angle (θ), and diameters of the filaments (D_W and D_L) as the spacer geometries [84].

The primary focus of feed spacer design research has been on the effect of spacer geometry on mass transfer and fluid dynamics in the membrane system. The purpose of changing the feed spacer's geometry is to lessen the impact of fouling on the membrane system without jeopardizing water production [22]. Li et al. [85] conducted one of the first evaluations in 2004 on unique spacer geometries, producing innovative spacers with enhanced filaments, twisted tapes, and multilayer

Fig. 3 Spacer configuration (a) nonwoven, (b) partially woven, and (c) fully woven. Reprinted with permission from Ref. [82], copyright 2022, IOP.

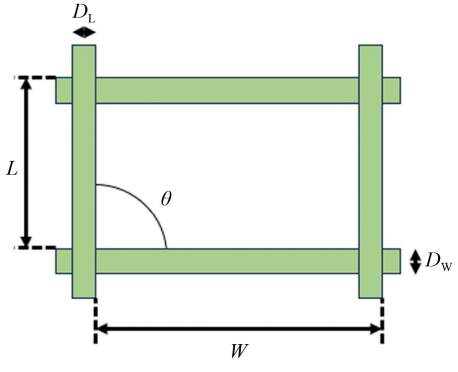

Fig. 4 Scheme of spacer geometry. Reprinted with permission from Ref. [84], copyright 2005, Elsevier.

structures. The best-performing spacer was determined to be the optimal multi-layer spacer with optimal non-woven nets in the outer layers and twisted tapes in the middle layer. The mass transfer study revealed that the multilayer spacer had a 30% higher Sherwood number and 60% lower power consumption than the commercial feed spacer [44].

Numerical investigations have also resulted in efficient spacer designs, geometries, and configurations. A study investigated the impact of commercial spacers with various thicknesses (28, 31, and 41 mil) on biofouling in the forward osmosis (FO) process and found that the thickest spacer provided the best performance with minimal biofouling and a flux decline recorded at 15% [86]. A similar finding was reported by Park et al. [15], who utilized a spacer with thicknesses of 28 and 34 mil. It was found that a thicker feed spacer with a thickness of 34 mil lowered membrane fouling, minimizing the frequency of membrane cleaning and extending the lifespan of the membranes. Mahdieh et al. [86], on the other hand, produced an optimized spacer with a filament thickness of 0.4 mm, and the optimized spacer produced 8% greater water flux than the standard 31-mil (0.86 mm) spacer under optimized conditions, as shown in Fig. 5.

A study by Gu et al. [82] investigated four different feed spacer configurations with 20 geometric modifications. 3D CFD simulations were used to investigate the effect of feed spacer design on membrane performance. Fully woven spacers produced the maximum water flux when built with a mesh angle of 60°, but the pressure drops are slightly larger than the nonwoven equivalents. The lowest water flux was produced by middle-layer geometries with a mesh angle of 30°. Meanwhile, spacers with a mesh angle of 90° exhibited the lowest pressure drop among all filament arrangements studied. Furthermore, the pressure is highly sensitive to the attack angle (the angle formed by the axial filaments and the direction of input) [82].

In recent years, a combination of both experimental and numerical investigations has been conducted to enhance the effectiveness of membrane filtration in terms of fouling and hydrodynamics [87]. Ali et al. [87] developed a column-type spacer by adding column-type nodes in the spacer structures. Additionally, 3D CFD simulations were used to numerically simulate the fluid flow behavior in the channel for this spacer, which was then compared to the conventional spacer. It was observed that the column spacer's specific flux was two times higher than the conventional spacer. The specific fluxes for the column spacer at 0.16 and 0.18 $m \cdot s^{-1}$ feed solution velocities were 101 and 95 $LMH \cdot bar^{-1}$, respectively. Meanwhile, the specific fluxes for the conventional spacers were recorded at 50 and 47 $LMH \cdot bar^{-1}$ of pressure drop across the test cell at the same velocities. Moreover, when a synthetic feed solution with a very high fouling potential was employed at the same velocities, the pressure drop

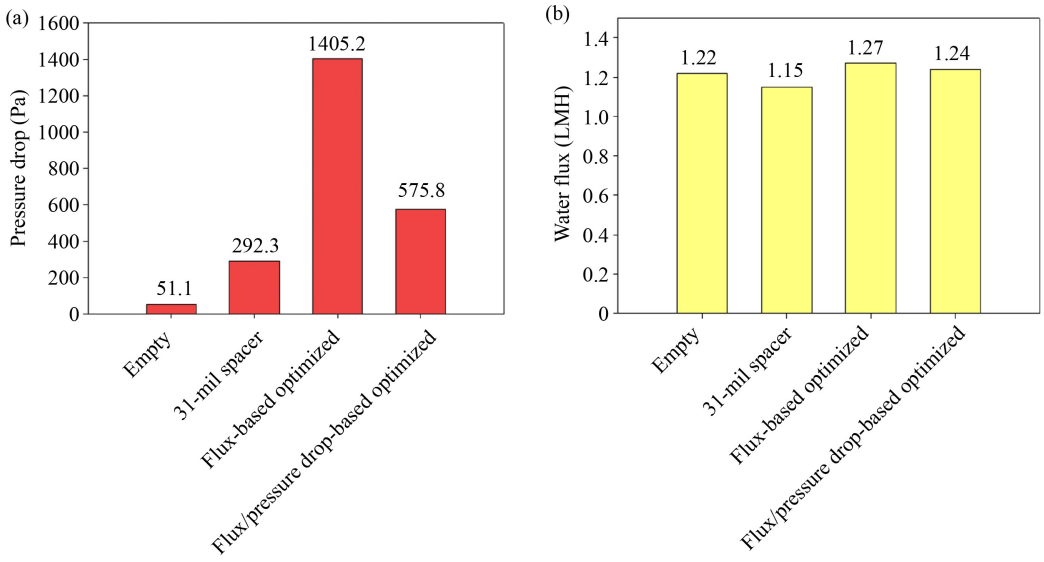

Fig. 5 Performance of different spacers under the same conditions applied in the optimization: (a) pressure drop and (b) water flux. Reprinted with permission from Ref. [87], copyright 2022, Elsevier.

for the column spacer was three times lower than that of the conventional spacer [87].

In 2020, Kerdi et al. [88] proposed novel feed spacers with a range of helices (1–3) along the spacer filament. At two distinct feed flow velocities (U_0 = 0.162 and 0.188 m·s^{-1}), the intrinsic effect of helices was experimentally explored to improve the permeate flux, reduce the pressure drop, and mitigate fouling. It was reported that the spacer with the most helices (3-helical) increased specific permeate flux the most (237% and 291% at U_0 = 0.162 and 0.188 m·s^{-1}, respectively), as shown in Fig. 6. Moreover, the performance of 3-helical spacers resulted in the greatest reduction in pressure drop, which was recorded at 65%, compared to 2-helical and 1-helical spacers, where the reduction in pressure drop was recorded at 55% and 46%, respectively. The significant low-pressure drop by the 3-helical spacer allowed the entire filtration module's energy consumption to be further reduced. The 3-helical spacers also demonstrated the highest increase in permeate flux and the most minimized fouling [88].

Qamar et al. [89] conducted a study comparing the performance of a non-woven commercial spacer, symmetric pillar, and hole-pillar spacer. The mentioned spacers were designed and developed using a 3D printer, as shown in Fig. 7. It was found that the hole-pillar spacer had a smaller initial channel pressure drop compared to the commercial spacer and pillar spacer, implying that the hole-pillar spacer consumes the least initial energy. On top of that, the hole-pillar spacer delivered the maximum

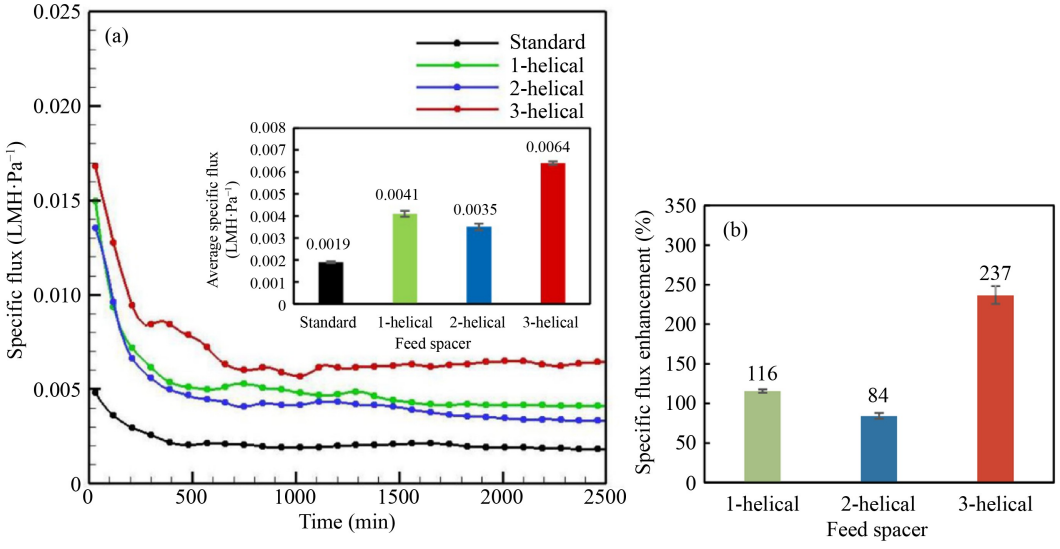

Fig. 6 Specific permeate flow (a) with average specific permeate flux at steady-state filtration (inset) and (b) percentage of flux recovery relative to the standard spacer as a function of the number of helices in the spacer's structure. Reprinted with permission from Ref. [88], copyright 2020, Elsevier.

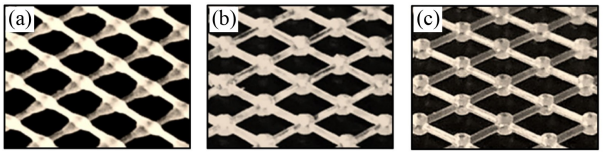

Fig. 7 3D-printed spacers (a) commercial spacer, (b) pillar spacer, and (c) hole-pillar spacer. Reprinted with permission from Ref. [89], copyright 2021, Nature Portfolio.

permeate flux regardless of applied pressure. The flux gain was 75% when P = 0.5 bar compared to the commercial spacer. However, the flux gain was reduced to 63% when P = 1.0 bar was used. The hole-pillar spacer also recorded minimized biofouling at all applied pressures, as the hole-pillar spacer had the lowest shear stress compared to the other two spacers analyzed [89]. Similar results were obtained by AlQattan et al. [90], where the hole-type spacer helped to boost the water flux slightly more than a regular spacer at the initial phase of the experiment. Moreover, at the end of the experiment, the pressure drop increased with the regular spacer but did not change with the hole-type spacer, which could significantly reduce energy consumption. The physical cleaning efficiency of a hole-type spacer was higher (100% flux recovery) than that of a standard spacer (95% flux recovery). This discovery was due to the presence of holes in the spacer filament intersections, which aided in the destruction and removal of the scaling layer on membrane surfaces, leading to improved overall operation [90].

In terms of spacer shapes, a novel honeycomb-shaped spacer is claimed to have the best-enhanced performance due to its structural merits as the most stable and economical structure in nature [91]. Park et al. [91] conducted experiments to compare the performance between honeycomb-shaped and diamond-shaped spacers. The outcome revealed that the honeycomb-shaped spacer significantly increases the permeate flux by 26.4% under heavy fouling circumstances compared to empty channel filtration. The results were also higher than those of the standard spacer, which showed an increase of 9.0%. Hydraulic cleaning studies showed that honeycomb-shaped spacers have a greater capability for overcoming fouling resistances caused by the CP layer and cake layer, resulting in increased permeate output compared to normal spacer filtration.

Ali et al. [24] developed a dynamic turbo-spacer to compare its performance with a diamond-shaped spacer of equal thickness. The diamond-shaped feed spacers employed in the membrane created excessive blockage in the channel, increasing flow unsteadiness and shear stress, causing foulants to accumulate in the constriction zone and increasing the pressure drop across the channel. The results showed that the turbo-spacer minimized fouling in a FO system and experienced a 15% lower flux decline compared to the diamond-shaped spacer, as shown in Fig. 8. The fouling effects also hampered turbo-spacer performance, but at a considerably lower rate. As illustrated in Fig. 6, the foulant resistance of the turbo-spacer at the end of the sixth cycle rose to 6.76 × 10^{13} m^{-1}, approximately 2.7 times less than the reference spacer [24].

Overall, based on the studies conducted previously, it is shown that specific geometric design, including the shape, thickness, and even the length of the spacer, impacts overall performance. A spacer that gives the highest accessible cross-section (voidage) possesses the lowest pressure loss and turbulence rates, and vice versa. With high turbulence rates, the concentration of polarization decreases, whereas the pressure drop increases significantly. As the pressure drop increases, the dead zones in spacer geometry are reduced, causing the tendency for the occurrence of biofouling phenomena to decrease as well [24]. More creative and efficient shapes have been fabricated in recent years and are expected to be further developed in the future to achieve the optimum design that can increase efficiency and reduce maintenance costs. With the help of new technologies such as AM, including 3D printing, the testing of the designs has become widely accessible, aiding in the progress and advancements of membrane spacers.

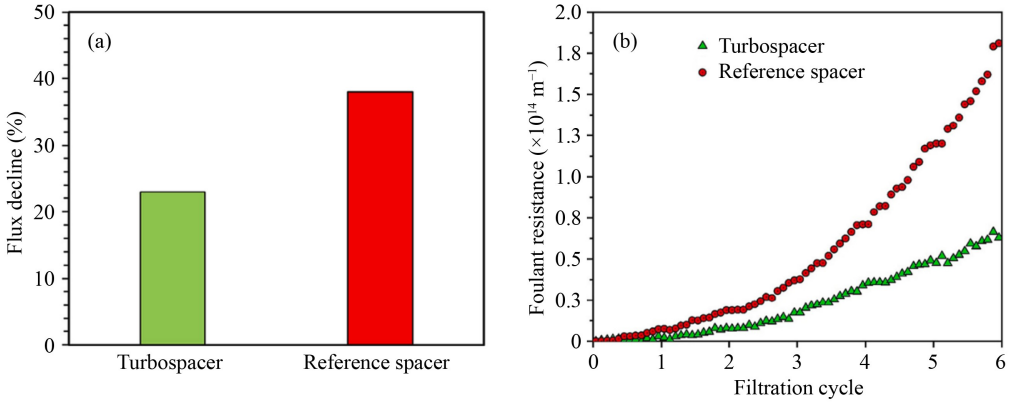

Fig. 8 (a) Flux decline (%) after the 6th filtration cycle and (b) transient foulant resistance (m^{-1}) during the FO operation using the turbospacer and the reference spacer (diamond-shaped spacer). Reprinted with permission from Ref. [24], copyright 2021, Elsevier.

3.2 Materials of spacer

As reported by other studies [6], the stagnation points in the spacer, caused by low velocity and recirculation, serve as the starting point for biofouling. The biofouling point then migrates and enlarges on the membrane surface. In addition to geometry, improving spacer material can help mitigate foulant accumulation, spacer fouling, and the increase in pressure drop in the membrane system. Traditionally, membrane spacers are designed with mesh-like structures created by extruding and welding low-density PP filaments. These spacers are chosen for their outstanding flexibility and chemical stability. However, exploring alternative materials with improved permeability and reduced resistance can contribute to better mass/heat transfer and lower energy consumption. Exploring new materials or surface modifications that promote favorable fluid flow characteristics can be highly beneficial for membrane filtration.

As a thermally driven process, membrane distillation needs to be modified in terms of the heat-transfer coefficient as well as mass transfer. Tan et al. [92] investigated the effect of the high thermal conductivity of two metals (nickel and copper) in metallic spacers used for direct contact membrane distillation (DCMD) via CFD simulations and experiments. The results revealed higher uniform temperatures along the feed-side membrane compared to the same system with PP spacers. Additionally, the lower heat loss rate and velocity on the membrane surface with metallic spacers caused a 16% improvement in the energy efficiency of distillate production with DCMD. The platinum-coated nickel spacer showed a better result, achieving a 28% reduction in the heater input energy per unit volume of distillate.

Another conventional method for improving the efficiency of spacers is coating PP spacers with various materials containing metals or metal oxides, polymers, and carbon-based materials. Metal oxides, specifically ZnO are suitable for inactivating bacteria and preventing biofouling due to the reactive oxygen species (ROS) generated in their presence. The ROS, containing hydrogen peroxide, hydroxyl, and superoxide radicals, can initiate lipid oxidation in the bacterial membrane, resulting in cellular damage and eventual cell death. Thamaraiselvan et al. [93] investigated the effect of metal oxide (ZnO, TiO_2, and SnO_2) nanorods' thin film coated on a PP feed spacer in a membrane filtration system. The first result revealed the negligible biocidal activity of TiO_2 and SnO_2 compared to ZnO in the dark. The mechanism proposed for the activity of ZnO nanoparticles involves binding zinc ions to the cell membrane, leading to bacterial growth inhibition. In addition, the nanorod coating with ODPA (octadecylphosphonic acid) was studied to enhance the anti-biofouling performance, with the results revealing a prevention of permeate flux reduction by more than 40% compared to the uncoated spacer. The superhydrophobicity of the ODPA coating layer (contact angle between 150° and 160°) caused bacterial repulsion from the spacer's surface and decreased bio-adhesion. Thamaraiselvan et al. [94] conducted another study focusing on the hydrophobic coating effect on microorganism growth in a membrane system. A thin layer of poly(dimethylsiloxane) was applied to the surface of commercial PP to enable feasible candle soot nanoparticles (CSNPs) coating. As a result of CSNPs coating, the superhydrophobic surface (contact angle higher than 150°) caused a signification reduction in biofilm growth (99% reduction) compared to the uncoated spacers.

Taiswa et al. [95] compared biofouling in an RO system between a PP spacer and a spacer coated with Cu and polydopamine-copper (PD-Cu). The study quantified biofilms using COMSTAT2 software with biovolume ($\mu m^3 \cdot \mu m^{-2}$) units. Less biofilm accumulation was observed on Cu and PD-Cu spacers with readings of 2.58 and 2.65 $\mu m^3 \cdot \mu m^{-2}$, respectively, while the control PP spacer showed a reading of 6.33 $\mu m^3 \cdot \mu m^{-2}$. The results confirmed that the Cu spacer reduced the biofouling rate by 41% biovolume compared to the traditional PP spacer. Aside from that, the permeate flux of the PD-Cu spacer outperformed the PP spacer by 17.5%. Tan et al. [96] conducted research on coating commercialized spacers with two hydrophilic monomers, acrylic acid and 2-hydroxyethyl methacrylate (HEMA), through a plasma-enhanced chemical vapor deposition method. Aside from significantly enhancing surface hydrophilicity, the HEMA-coated spacer showed a higher flux recovery rate (94.17%) and salt rejection (95.78%) for the RO membrane compared to the commercialized spacers with an 89.44% flux recovery rate and 92.46% salt rejection, respectively. Moreover, the HEMA-coated spacer exhibited significantly better antifouling properties, with a fouling layer that was thinner (200 nm) compared to the commercialized spacer (700 nm). Based on Table 1, different coatings can affect membrane systems in terms of biocidal properties, anti-biofouling performance, and permeate flux.

Modification of the spacer's material against biofouling by mixing it with nanomaterials is another area of material research on membrane spacers. Kitano et al. [103] studied the organic antifouling properties of mixed carbon nanotubes (CNTs) and compared them to conventional PP nanocomposite spacers using an injection molding system. To investigate the fouling resistance of PP/CNTs spacers, different concentrations of CNTs (from 5 to 15 wt %) mixed with PP were compared with a plain conventional PP spacer in a cross-flow RO system with a solution containing bovine serum albumin (BSA) protein and NaCl salt. Their results revealed that after 144 h of membrane operation, the

Table 1 The coating layer effect on the membrane spacer efficiency

Material	Coating	Membrane system	Bacteria	Mechanism	Efficiency	Ref.
PP	ZnO nanoparticles	UF	*Pseudomonas* (*P.*) *putida*	ROS generation	Permeate flux improves by at least 50%	[97]
PP	Nanosilver	UF	*P. putida*	ROS generation	~45% permeate flux improvement in 10 d	[98]
PP	PolySPMA	NF/RO	*E. coli*	Hydrophilicity, charge interaction	~50% reduction in bacterial attachment after 24 h	[99]
PP	Ag nanoparticles poly quaternary ammonium	UF	*P. putida*	ROS generation Charge interaction	Near 3 times higher permeate flux after 10 d More than 2 times higher permeate flux after 10 d	[100]
PP	ZnO nanorods ODPA	–	*B. subtilis* *P. putida*	ROS generation Hydrophobicity	80% reduction of total bacterial attachment 92% reduction of total bacterial attachment	[93]
HDPE/PP	Poly(sulfobetaine methacrylate)	RO	*P. fluorescens*	Antifouling agent	70% biofouling reduction in 24 h	[101]
PP	CSNPs	RO	*P. aeruginosa* *Cobetia marina*	Hydrophobicity	99% reduction in biofilm growth	[94]
PP	Laser-induced graphene	RO	*P. aeruginosa* *Rheinheimera* sp.	An electrical circuit, charge interaction, ROS generation	93%, 66%, and 49% reduction of live bacteria in the front, middle and back part of the spacer, respectively	[102]
PP	Vanillin	RO	*E. coli* *S. aureus*	Quorum quenching and hydrophilicity	96.7% and 64.3% reduction in the colonies' number	[26]
PP	PD-Cu	RO	*E. coli*	ROS generation	17.5% higher permeate flux and a 58% biofilm biovolume decrease in 24 h (nak buang)	[95]

PP/CNTs nanocomposite spacer exhibited superb antifouling capability against BSA compared to the plain conventional PP spacer, due to the reduction of roughness in the novel spacer and changes in electrostatic interaction.

With the development of 3D printing technology in recent years, the performance of membrane spacers has improved in various fields. Compared to PP-made spacers, most 3D printed spacers, such as ABS, polyamide (PA) 2200, and acrylic-based monomer, demonstrate better flexural performance due to the higher strength and elasticity of the materials [23]. The material classification of 3D printing, including solid, liquid, and powder-based, has all been used in membrane spacer research. Based on the research by Ibrahim and Hilal [104], the 3D-printed spacers are around 47% liquid-based, 36% powder-based, and 17% solid-based. The liquid-based technique is primarily based on photo-polymer resins. However, solid and powder-based 3D printing can be done with thermoplastic, metallic, and ceramic materials.

Yanar et al. [105] investigated the effect of different materials (ABS, PP, and natural PLA) on PolyJet 3D printed spacers in FO membrane systems and compared them to a commercial PP (Com) spacer as a reference. The results revealed that the water flux of the ABS and Com spacers was comparatively higher than that of PP and PLA spacers (in the order of ABS > Com > PP > PLA). Based on Fig. 9, the highly smooth surface was reported as the reason for the higher water flux in the system with ABS and Com spacers. Although PLA also has a smooth surface, the relatively smaller hole area caused a slight difference in water flux compared to the spacers mentioned above (PLA 6.19 LMH, Com 6.62 LMH, ABS 6.99 LMH).

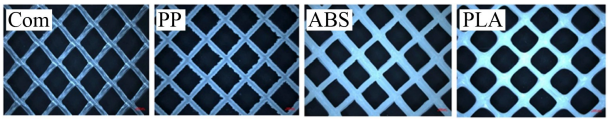

Fig. 9 Images of a stereo fluorescence microscope showing the following spacers: Com, PP, ABS, and PLA. Reprinted with permission from Ref. [105], copyright 2018, Elsevier.

Furthermore, alginate-based wastewater was utilized in the fouling test, and the system with the PLA spacer showed nearly 10% less fouling than the Com spacer. Based on this improvement, they concluded that the natural biopolymer PLA could be a comparable choice for further investigation. In 2021, the same team studied the modification of PLA-based spacers with electrically polarized (E-GRP, graphene-polylactic acid) and non-polarized (GRP) graphene in an FO membrane system [106]. The 3D printing method they used was the fused deposition modeling (FDM), so the PLA in these studies was a solid-based filament, and the ratio of graphene to PLA in the modified filaments was 8%. The results showed that the water flux improved significantly from the system with PLA (20.8 ± 2.1 LMH) or GRP (20.5 ± 2.3 LMH) draw spacers to the system with E-GRP (32.4 ± 2 LMH) due to the higher surface electrostatic charge of the spacer after polarization. In another research, they investigated the effect of these spacers on fouling caused by calcium chloride and a sodium alginate solution. They concluded that the FO system with polarized graphene had 70% less fouling than the other two, resulting in a 14% water flux decrease after the 5 h test, which was better than the 31% and 33% water flux reduction observed in the system with PLA and non-polarized graphene, respectively.

A study by Ibrahim and Hilal [107] was conducted using

3D-printed feed spacers made of poly(ether sulfone) (PES), which were printed directly on a fabricated membrane. The 3D-printed PES feed spacer was produced with various concentrations of PES polymer (18, 20, 22, 25, and 28 wt %) to observe the effect of solution viscosity on 3D printed pattern fidelity and the membrane performance. A conventional flat membrane with a 3D printed non-porous PLA spacer is used as a comparative reference. The findings showed that the modified 3D-printed feed spacer integrated into the membrane increased pure water flux by 31.0%–130% compared to the utilization of traditional plastic feed spacers. However, the viscosity of the 3D printing solution significantly affected the spacer's performance, where low-viscosity solutions exhibited lower printing accuracy. The concentration of PES polymer at 18 wt % (P18) had the lowest viscosity, and the pattern of the spacer tended to flatten during printing, which significantly reduced its performance. P18 even showed the lowest antifouling properties in the antifouling test compared to the other concentrations, which exhibited superior antifouling performance [107]. Table 2 shows some examples of using 3D-printed spacers in membrane systems.

The study of materials for membrane spacers is still in the exploration stage. The potential effects of different materials on the performance of membrane spacers in various membrane processes are fascinating. With the increasing use of 3D printing in the membrane technology field, the options and studies on materials have become broader, as different 3D printing materials for spacers offer different finishes and performances. Additionally, the blending of nanomaterials with 3D printing materials has yet to be deeply studied, and the

Table 2 Summary of 3D-printed spacers in membrane systems

Material	Material type	3D printing method	Membrane system	Pollutant solution	Mechanism	Efficiency	Ref.
PA 2202 (thermoplastic powder)	Powder	SLS	DCMD	Calcium sulfate	Improvement in design and thus flow hydrodynamic	50% flux increase	[108]
PA 2202	Powder	SLS	DCMD	Humic acid	Improvement in design and thus flow hydrodynamic	Flux enhancement by 50%–65%	[109]
Acrylate monomer (BV-007)	Liquid	DLP	UF	Bacto^{TM} yeast extract, sodium alginate, xhantan gum	Column shape design of the spacer	3 times lower pressure drop, 50% less flux decline after 48 h	[87]
PA 2202	Liquid	SLS	UF	Sodium alginate, calcium chloride	Improvement in spacer design	Inhibit the cake formation on the membrane	[110]
VeroClear (PMMA)	Liquid	PJM	RO	Sodium chloride, silica particles	Improvement in spacer design	Improvement in inorganic fouling and biofouling	[111]
VisiJet® M3 crystal	Liquid	MJM	MF	Glycerol, xanthan gum, plasma mimicking solution	Changing the flow hydrodynamic due to the addition of spacers	Flux enhancement, fouling reduction	[112]
PA, fluorinated silica	Liquid	SLS	MD	Calcium sulfate	Microscale roughness and hydrophobicity	74% decrease in the scalant attachment on the spacer, 60% less scale deposition on the membrane	[113]
PA 2202	Liquid	SLS	MD	Deionized and tap water	Improvement in spacer design	17% flux reduction improvement, 50% lower pressure drop	[114]
Acrylate monomer (BV-007)	Liquid	DLP	FO	KAUST wastewater, sodium chloride	Improvement in spacer design	Near 15% flux reduction improvement, 2.5 times lower foulant resistance	[24]
PES, graphite, silver NPs	Solid	FDM	UF	Humic acid, sodium chloride	Electrical conductivity and bubbling, direct integration of spacer and membrane, spacer design and turbulency	Flux improvement, self-cleaning ability	[115]
VisiJet crystal (photosensitive resin)	Liquid	PJM	NF	Magnesium sulfate	Improve in spacer design	More than 69% reduction in the energy cost	[116]
Photopolymer resin, PVDF	Solid	FDM	UF	Humic acid	Improve in design and turbulency	Reduced fouling, nearly 150% higher flux	[115]
PLA	Solid	FDM	FO	Olive oil, sodium dodecyl sulfate	Improve in design and turbulency	20% increase in flux, improvement in fouling resistance	[117]
PlasCLEAR photopolymer, $Ti_3C_2T_x$ MXene	Liquid	DLP	MD	Sodium chloride	Photothermal conversion effect of the MXene	Near 100% increase in water flux, 85% improvement in energy consumption	[118]
PLA, CNT, graphene	Solid	Fused filament fabrication (FFF)	MD	Sodium chloride	Turbulence due to the formed roughness	43% and 75% increase in permeate flux using 1% graphene and 2% CNT, respectively	[119]
Acrylate monomer	Liquid	LFS	UF	Bacto^{TM} yeast extract	Improvement in the spacer design and the local hydrodynamics inside the filtration channel	228% enhancement in permeate flux, 23% reduction in specific energy consumption, and 74% biofouling development	[120]

possibilities are promising. The main challenge in blending these components is attaining a uniform nanomaterial distribution in the polymer matrix, since agglomerations of the nanomaterials could lead to reduced material properties. Furthermore, the selection of nanomaterials to be blended in the 3D matrix is crucial, since the compatibility of interactions between the nanomaterials and the matrix must also be considered.

4 3D printed membrane spacer

The fabrication of membrane spacers can be conducted through traditional methods or the emerging technology called AM, specifically the 3D printing method. Common traditional methods include injection molding, extrusion, and casting, which are suitable techniques for spacer production, as most spacers are made of thermoplastics. Although traditional methods have been established and refined over time, more studies are focusing on the promising possibilities of 3D printing. These traditional methods often involve significant tooling expenses, longer time consumption for mold creation, and limited flexibility in rapid design or customization, where geometries are restricted to conventional ladder- and net-type structures [23].

Research on spacer fabrication favors the 3D printing method nowadays, with most studies focusing on alternatives to improve the efficiency of spacers by reducing fouling phenomena. In general, 3D printing is defined as an emerging method that creates parts from 3D pattern data by utilizing layer-by-layer jointing of material, showing promising applications in water and wastewater treatment, biomedical fields, automotive, aerospace, building, and food industries. The 3D printing method can produce porous materials with complex geometries. Aside from the convenience that comes with the utilization of 3D printing, the method itself offers various advantages in sustaining the raw materials of the spacers by reducing the amount of material used for their development and production.

3D printing has become significant in various fields, and various 3D printing methods are slowly being introduced to ensure the flexibility of using different materials. Despite the various options in methods, choosing the most suitable method that is compatible with the material while improving the properties of the fabricated products remains a challenge. Thus, the need for more studies in the 3D printing field is evident. While traditional methods are still widely used in the industry due to their reliability, 3D printing methods are still being progressively researched and may replace traditional methods in the future. In this review, different types of 3D printing methods are discussed to provide a clear view of their advancement.

4.1 Selective laser sintering (SLS)

One of the significant AM techniques is SLS. Compared to traditional techniques such as nonsolvent-induced phase separation and thermally induced phase separation, which are commonly utilized due to their simplicity and ease of scale-up, SLS offers more control over the membrane structure. It provides enhanced control over fouling, lowers production costs, and prevents environmental problems by eliminating the usage of solvents while maintaining high accuracy and strength.

The schematic diagram of the SLS method is shown in Fig. 10. In the SLS process, laser power heats solid polymeric particles (powder bed) to melt and lower the viscosity of the particles, allowing them to fuse with the membrane (step [3] in Fig. 10). The laser is typically a carbon dioxide laser used in an inert gas atmosphere. When the molten polymer cools, it forms a firm sticky layer on the membrane. After consolidation, shifting the right piston down lowers the powder bed by the thickness of a new thin layer (step [4] in Fig. 10). Then, new powders are spread over the current deposit (steps [1] and [2] in Fig. 10), and this cycle is repeated several times. This method of 3D printing does not require support since the remaining unsintered powder bed can hold the printed model in place. Moreover, this method can result in high accuracy for the finished product, since the powder bed does not move throughout the printing process. Nevertheless, the excess powder can be eliminated by ultrasonic cleaning [121] or a sandpaper brush [122].

Polymers have been widely utilized for the powder bed due to the low processing temperature, low laser power, and high dimensional accuracy of the printed parts [123]. Polymers are generally categorized into three types: thermoplastics, thermosets, and elastomers. Thermoplastics, such as polycarbonates and PA, are the most common polymers in the SLS process due to their high

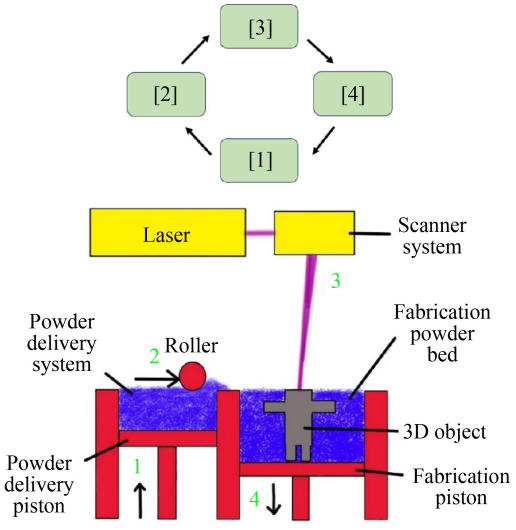

Fig. 10 Schematic of SLS.

mechanical properties, stability, chemical resistance, and excellent recyclability [124,125].

Some parameters have a significant impact on the fabricated membrane structures. Yuan et al. [126] manipulated three different process parameters: laser power, hatch spacing (distance between laser tracks), and scan count to optimize the PA-12 microfiltration membrane performance. PA-12 is one of the most popular materials for the SLS process. They reported that laser power is directly linked with rejection and pure water flux, and the optimum value was 0.1 $J \cdot mm^{-2}$. They also mentioned that the membrane structure would be denser with higher energy density, a smaller distance between laser tracks, and two laser scan counts. In another study, Tan et al. [127] investigated SLS processing parameters such as layer thickness, part bed temperature, energy density, and scan pattern for successfully fabricating net-typed PP spacers. PP is a commercially used material for feed spacers due to its flexibility in being rolled up around the central permeate tube, low cost, and excellent chemical resistance properties. They found that a higher energy density can lead to a higher Young's modulus and, consequently, higher strength of the printed net-typed tensile bars, consistent with those reported by Yuan et al. [126]. Additionally, favorable results for strength and net tensile structures included small dimensional variations. Yang et al. [128] reported that aging is another critical parameter, noting that the microstructures of parts using aged PA 12 powders were coarse spherulites and showed degraded surface morphology, yielding rougher surface smoothness compared with parts from new powders.

Al-Shimmery et al. [129] fabricated a composite with a thin selective layer of PES onto an ABS-like support with flat and wavy structures via 3D printing to filter an oil-in-water emulsion. The results showed excellent performance of wavy structures in terms of permeation and cleanability, with the pure water permeance and permeance recovery ratio through the wavy membrane being 30% and 52% higher than those of the flat structure, respectively. Additionally, the wavy structure exhibited low irreversible fouling and a slow fouling formation rate, reducing operational costs and the need for environmentally harmful chemical cleaning. Simultaneously, both flat and wavy structures demonstrated an oil rejection of 96%.

Yuan et al. [130] coated CSNPs on a polymer membrane via SLS method. The fabricated membrane showed hydrophobic stability after 30 min of sonication, underwent solvent treatment for 7 d, and exhibited high separation efficiency (99.1%) for the oil/water separation mixture. Another application of SLS is shaping commonly used biomass such as chitosan and cellulose. In conventional methods, chitosan was dissolved in solvents and acids, which are harmful to the environment, and then fabricated into the membrane. Sun et al. [131] formed a membrane from chitosan by mixing SLS with thermoplastic polyurethane. The hybrid membrane demonstrated the ability to adsorb heavy metal ions, with maximum adsorption capacities of 19.6 and 30.4 $mg \cdot g^{-1}$ for Cu(II) and Pb(II) ions, respectively. This demonstrates the flexibility of the sintering method with increased functionalities.

4.2 Digital light processing (DLP)

The main limitations of the 3D printing method include the cost of the equipment. Among the various 3D printing methods, DLP stands out for its advantages of low equipment cost, accuracy, and high production rate. However, it has the disadvantage of being limited to using a single material [132].

In this method, projected light or UV rays cure the liquid resin through the polymerization of the liquid resin contained in a vat, which changes its physical properties upon exposure to the laser beam. The liquid resin should be photo-curable and stable with optical transparency. The beam is projected onto a fluoroplastic film fitted at the bottom of a vat, allowing it to harden through polymerization and chemical reaction. This process is done layer by layer from the top to the bottom of the product, with the dimensional height of each layer ranging between 0.01 to 0.2 mm. A platform is required during the process to keep the object stable. The schematic of DLP is demonstrated in Fig. 11. Acrylate monomer and photopolymer resins can be used as liquid resins; however, acrylate monomer benefits from higher resolution, with a fine layer height of 50 mm. The resolution of the product is defined by the number of pixels [87].

Some parameters have an impact on the fabricated membrane structure in DLP. Kim et al. [133] produced fabrics using DLP with a polyurethane acrylate photopolymer as the printing material. They investigated parameters such as curing time and layer thickness to control the physical properties of a printed model, including tensile strength, elongation, and crease recovery. They found that the optimum parameters were 10% (v/v) concentration of acrylate oligomer in the

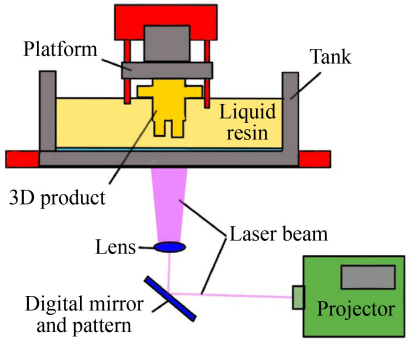

Fig. 11 Schematic of DLP.

photopolymer, 14 s of curing time per layer, and a layer thickness of 100 μm. In another study, Riahi et al. [134] fabricated a corner array retro-reflective structure using the DLP method. They also investigated the effect of layer thicknesses on the surface of the cube. They reported that the optimum roughness was obtained at an orientation of 54.7° around the *y*-direction and 45° around the *z*-direction.

Additionally, Monzón et al. [135] showed that the build direction significantly impacts the mechanical properties, as shown in Fig. 12. According to them, the vertical build direction provides better mechanical properties than the horizontal one. This premise is due to the adhesion between layers, where the vertical build direction provides strong adhesion. Another reason that contributes to this premise is based on the resolution of the DLP technology, where the entire layer is not entirely cured, leaving small areas between each pixel.

Li et al. [85] investigated different geometries to enhance mass transfer in membrane spacers. The results indicate that the mass transfer performance of the optimally designed multi-layer spacer with non-woven nets in the outer layers and twisted tapes in the middle layer (Fig. 13) was identified as the best-performing spacer, with the Sherwood number about 30% higher and power consumption roughly 40% lower than the other geometries.

Chen et al. [136] have introduced a novel method for preparing high-flux ceramic membranes by dispersing alumina in a photosensitive resin to form a UV-curable slurry for the DLP technique. The manufactured ceramic membrane showed a uniform pore size distribution, a low tortuosity factor, high porosity, an asymmetric structure, and high permeate flux. This fabrication method can be applied to the production of membrane spacers, where the water flux of such spacers can be analyzed and further improved.

4.3 Polyjet

Photopolymer jetting, or Polyjet, as shown in Fig. 14 [137], is one of the 3D printing methods that uses photosensitive resin in liquid form. The printing of the 3D object is done layer by layer on a platform through the deposition of resin dispensed from the inkjet nozzle in the form of droplets. This technology implements the principle of UV curing, where the final product is cured and solidified instantly by subjecting it to UV rays [14,138,139]. Three main steps are involved in this type of printing: pre-processing, processing, and post-processing. The pre-processing focuses on optimizing the part orientation on the build tray. For the processing step, the inkjet print head deposits droplets of resin onto a built tray, and each layer is cured by UV light. The process progresses with the building tray moving down layer by layer until the part is entirely fabricated. The post-processing step involves removing the support material using a water jet recycling station [137]. The printing

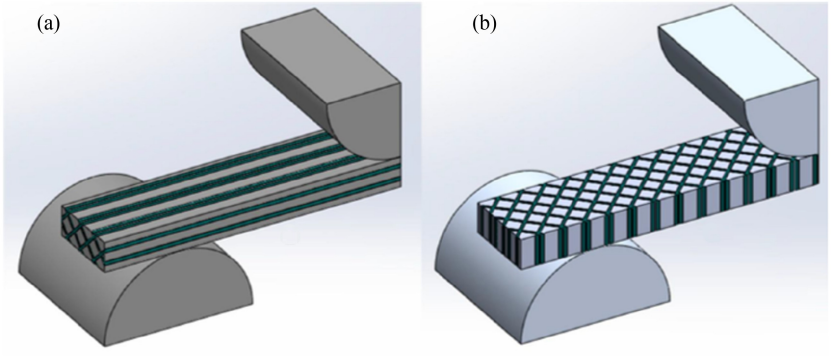

Fig. 12 Samples made under (a) vertical direction and (b) horizontal direction. Reprinted with permission from Ref. [135].

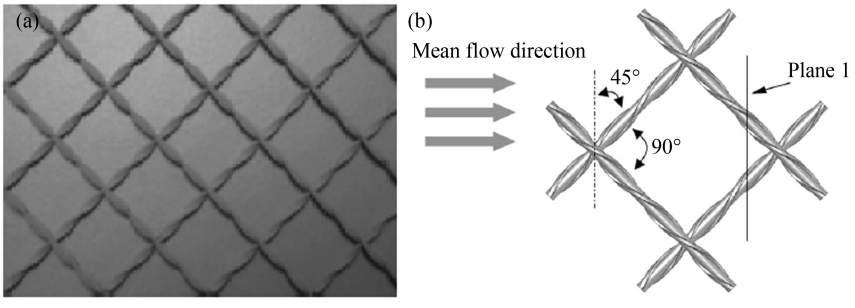

Fig. 13 (a) The twisted tapes spacer manufactured, (b) Longitudinal vortices in a flat channel. Reprinted with permission from Ref. [85], copyright 2005, Elsevier.

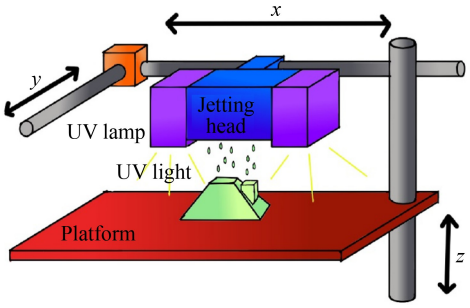

Fig. 14 Schematic diagram of Polyjet printing method.

materials commonly used for this process are photopolymers such as PP [105,140] and acrylic-based monomer [141]. The Polyjet technique provides high resolution and accuracy, making it suitable for printing small and delicate objects with a smooth surface finishing [14,132].

To date, it has been shown that the Polyjet 3D printing technique is the most effective method to fabricate membrane spacers. A study comparing spacers produced by different printing techniques was conducted by Siddiqui et al. [139] in 2016. It was demonstrated that the Polyjet 3D printing technique is the most effective method for fabricating spacers with higher resolution compared to FDM and stereolithography (SLA) printing techniques. Spacers produced using FDM and SLA were found to be brittle, deviated from the intended design, and exhibited lower mechanical strength [139]. This could lead to low membrane filtration performance during the application.

Additionally, Tan et al. [141] also demonstrated that spacers fabricated using the Polyjet technique had better performance compared to FDM and SLS. While all the spacers showed improved performance compared to a commercial spacer in terms of mass transfer at fixed power consumption and critical flux, the Polyjet 3D printed spacer exhibited the most accurate design based on the intended design, while FDM showed the highest deviation. Additionally, the semi-anisotropic surface finish of Polyjet was found to have a significant effect on critical flux.

Siddiqui et al. [139] conducted a comparison between a conventional spacer and a spacer fabricated using the 3D Polyjet technique with similar geometry. The results indicated that both spacers exhibited the same biomass accumulation, hydrodynamic behavior, and pressure drop. However, when the study altered the design of the 3D-printed spacer, the modified 3D-printed spacer demonstrated a lower pressure drop over time, and the biomass accumulation was reduced.

Another study by Lam et al. [142] involved the fabrication of three spacers using Polyjet techniques with different materials and compared them to a commercial spacer. The results revealed that the spacers fabricated using PLA exhibited the highest precision compared to the 3D CAD model, while the spacer fabricated using ABS showed the highest deviation. This may be caused by the swelling behavior of the ABS material, which promotes invisible porosities after printing and increases the thickness of the ABS spacer. Nevertheless, all the spacers demonstrated better performance for reverse solute flux and fouling resistance compared to the commercial spacer, and both showed similar water flux [105].

Based on the studies, the Polyjet 3D printing method could be a good option for fabricating spacers, provided that the geometric design and materials used alongside the Polyjet method are suitable for spacer fabrication. However, despite the potential of Polyjet 3D printing in membrane spacer technology, the printers and materials for this technique are expensive, the strength of the produced parts is considerably low, and the process of removing supports and cleaning up is rather complicated [14,132].

4.4 FDM

FDM, or FFF, is an extrusion-based 3D printing method commonly preferred among AM processes [143]. This method involves a rapid prototyping process where each new layer is created by extruding a filament of wax or polymer onto the existing part surface from a work head to fabricate a 3D structure [144]. The filament is extruded based on the CAD design, with the bed moving down or the nozzle head moving up following the required layer thickness, and each new layer is built onto the previously solidified layer [145]. As shown in Fig. 15 [146], the FFF process starts by heating the thermoplastic filament held by the printer's print head until it melts.

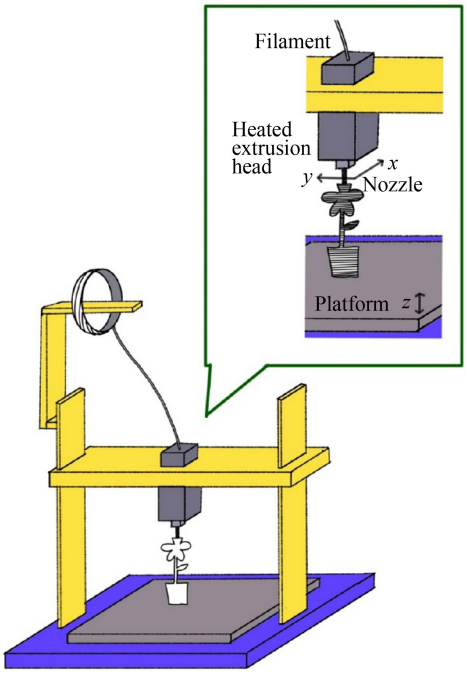

Fig. 15 Schematic diagram of the FDM printing method.

The melted filament is then extruded through a nozzle that moves along the *X*, *Y*, and *Z* axes according to the instructions while depositing the melted filament layer by layer to build up the object. Each layer cools down and solidifies rapidly, after which another layer is deposited, and the layers bond with each other. Once the prototype has been fully printed, it is left to cool and harden completely before being removed from the build platform.

This technique has been favored by academicians, researchers, and industrialists due to its simple fabrication process, reliability, smooth operation, ease of removing support material, good raw material handling, ability to utilize different thermoplastics, dimensional stability, low maintenance, cost-effectiveness, and the ability to fabricate products with high resolution [145]. Even so, this technique has many limitations and issues that are being studied and improved. One of the issues is the reduced mechanical strength of the products due to the weak interfacial bonding strength and porosity of the printed objects [143,147,148]. Aside from that, the performance and fuctionality of the printed parts are highly affected by various parameters, including extruder geometry, processing parameters (such as the hot melt and hot bed temperatures, and printing speed), and workpiece depositing parameters (including the number and thickness of layers, infill geometry and density, number of layers, raster angle, gap, and width patterning) [143,149−151].

Yanar et al. [79] conducted a study focusing on the performance of 3D-printed electrically polarized graphene-blended PLA spacers produced through the FDM technique. Three types of spacers (PLA spacer, graphene-blended spacer, and electrically polarized graphene-blended spacer) were successfully produced, and the water flux and alginate fouling of the spacers were relatively similar. In a related study, Yanar et al. [106] fabricated an electrically polarized 3D-printed spacer utilizing a graphene blend using the FDM 3D printing technique. Although the spacer had been successfully fabricated according to the CAD model, a marginal difference in terms of thickness was observed, with the spacer showing a lower thickness compared to the CAD model due to the limited resolution of the FDM 3D printing process. This observation aligns with a study by Siddiqui et al. [139], where the researchers developed a strategy to design and evaluate feed spacers with a modified geometry for spiral-wound NF and RO membranes. The resulting 3D spacer membrane developed using various 3D printing techniques was benchmarked with a commercial feed spacer. The study concluded that FDM is not a suitable technique for producing feed spacers, as the spacers produced were thicker than the commercial feed spacer, and they exhibited brittleness during application. Additionally, Yanar et al. [106] found that the strength of the melted filament used for producing the spacer using the FDM technique is not optimal. However, rigidity and precision increase when the spacer is blended with graphene.

According to another study, FDM-based materials have a rough surface finish [152]. Spacers produced using the Polyjet technique have shown a smoother surface finishing compared to the spacer produced by FDM [139], although the Polyjet technique is more costly [14,132]. Nonetheless, chemical treatments can be used to improve the surface quality of FDM parts. Various studies have been conducted in the past to enhance the surfaces of FDM parts, and it has been observed that most studies can improve the surface by dipping it in acetone or treating it with the hot or cold vapor of acetone. Recent studies have also used dichloroethane for the dipping process. While a decrease in surface roughness increases the ductility of the material, it may reduce tensile strength [153].

There are various 3D printing methods, and it is significant to choose the method based on the desired application. Fabricating spacers requires precise and smooth geometries to optimize flow behavior. One of the significant factors of choosing 3D printer for spacer is its accuracy in printing complex and detailed geometries. Table 3 shows the resolution range and accuracy of 3D printers. Based on the table, DLP shows the highest resolution, with an accuracy range of 10–25 µm, which makes it the ideal for complex and high-precision designs. The Polyjet printer offers excellent accuracy as well, ranging from 10 to 20 µm, making it suitable for printing highly detailed components with smooth surface finishes. On the other hand, SLS provides low accuracy at 300 µm, which is insufficient for precise spacer design. FDM has the lowest accuracy at 350 µm, which makes it difficult to print an efficient spacer with optimized flow patterns [154].

4.5 Advancement of 3D printed membrane spacer

AM is still a relatively new technology in the area of water treatment and requires further improvement to make it feasible for implementation in the industry.

Table 3 Resolution range and accuracy of 3D printing methods [154]

Methods	Resolutions range (µm)	Accuracy (µm)
SLS	*x*: 50	300
	y: 50	
	z: 200	
DLP	*x*: 25	10–25
	y: 25	
	z: 20	
Polyjet	*x*: 30	10–20
	y: 30	
	z: 20	
FDM	*x*: 100	350
	y: 100	
	z: 250	

Balogun et al. [155] have suggested several aspects that can be improved, including reducing the surface roughness of the 3D-printed spacer through post-treatment to reduce biofouling. The number of publications related to 3D printing for various applications, including membranes and spacers, has developed at a fast pace in recent years. Thus, there is a need to carefully analyze the latest developments in 3D-printed membranes and membrane spacers. As of now, 3D printing has been used in the production of membrane spacers at the research level and has not yet been marketed commercially. 3D printing is a very promising approach in developing membrane spacers. However, it still prototypes spacers at rates much slower than traditional methods, which typically involve injection mold tools that require expensive investments.

As the membrane industry still utilizes conventional manufacturing methods to produce membrane spacers, 3D printing is beneficial for verifying a design by prototyping the spacer and testing it before investing in an expensive molding tool, an approach that is far cheaper than redesigning or altering an existing mold [156]. In addition, it is easier to manufacture the spacer in small batches using a 3D printer rather than producing it in larger batches. 3D printing also has the capability to create complex designs that traditional manufacturing is not able to achieve. Moreover, 3D printing offers various advantages in producing spacer membranes, including design freedom, where the geometric design of the spacer can be manipulated according to preferences and suitability, the ability to produce complex designs, and cost-effective and low-volume production.

Many studies have proven that 3D printing can produce parts for various applications, but this technology still faces several challenges that require further improvement. Prototyping 3D-printed parts, including spacer membranes, is limited by printing resolution, leading to problems in the feasibility of 3D printing for wastewater treatment. Moreover, there are challenges regarding upscaling the production due to the small build volume and slow printing speeds [21]. Most manufacturers still use conventional methods to produce spacers because of the limitations of 3D printing in mass production. A product can only be 3D printed one at a time by a single 3D printer. Mass production via 3D printing may consume significantly more time than production using conventional methods [64], making it currently economically unfeasible. Even though several research and applications have been conducted to implement large-scale 3D printing [157,158], the implementation is still new and needs improvements, as current capabilities are limited to meter-scale fabrication. The trade-off between accuracy and efficiency is apparent when compared to the conventional 3D printing technique. While bulk production of spacers may be possible, the requirements for various post-processing, material performance optimization, equipment refinement, and precise printer control still need to be taken into consideration. The size effects of production would likely have effects on uniform distribution in terms of shape, accuracy, quality, and performance [159].

The production cost of a membrane spacer is highly dependent on the fabrication methods. Due to a lack of information, determining the exact details of the production cost for a membrane spacer using either conventional or 3D printing methods is generally challenging. Calculating the cost of 3D printing as a capital expenditure (CAPEX) is also difficult due to the rapidly evolving nature of the technology and the wide variation in printer types, materials, and economies of scale. For example, the cost of 3D printer resin for SLS printer cost between 200 and 300 $\$\cdot kg^{-1}$ in 2017, whereas the cost for filaments for FDM printer was around 250 to 350 $\$\cdot kg^{-1}$ [160]. However, by 2020, the cost of 3D resins and filaments for SLS and FDM printers had dropped as low as 20 and ~50 $\$\cdot kg^{-1}$, respectively [114]. The implementation of material-reuse methods has significantly aided in cost reduction by 10% and 70%–80% for SLS and FDM per part [161]. In terms of printer type, a consumer-grade 3D printer could be retrieved with a cost as low as $500 (with lower resolution), while a high-resolution industrial-grade printer can cost up to $1 M [114].

Thomas et al. [114] had conducted a cost analysis on the cost-effectiveness of 3D-printed membrane spacers in air gap membrane distillation (AGMD) and DCMD systems, taking into account water flux, energy efficiency, and pressure drop. The geometry design of the 3D-printed membrane spacer used in their research was based on triply periodic minimal surfaces (TPMS), which improve mass transfer and reduce pressure drop, mainly in AGMD. The study calculated the cost of water (COW), involving CAPEX (membranes modules and spacer cost), and operating expenses (OPEX: pumping energy, thermal energy, and labor). Based on the report, a small-scale AGMD system (10 $m^3\cdot d^{-1}$) using the 3D-printed TPMS spacer reduced COW by 9.2% with additional heat costs. On the other hand, a large-scale AGMD system (1000 $m^3\cdot d^{-1}$) manages to reduce COW by 8.9% under similar conditions. However, in DCMD, even though the pressure drop increased, the flux gains could offset this, though they cause disadvantages in the economic profile. Utilizing 3D-printed spacers results in higher CAPEX due to elevated per-unit manufacturing costs compared to traditional spacers. However, the OPEX has the potential to be significantly reduced, mainly due to flexible and detailed designs like TPMS design, which reduces pressure drops significantly and leads to reduced pumping energy. Additionally, the designs offer enhanced hydrodynamics, which contributes to a higher water flux and reduces the thermal energy required per unit volume of treated water. The research concludes that as the plant

size increases, the overall CAPEX per unit volume of treated water might decrease due to economies of scale. However, the manufacturing cost of membrane spacers may become significant in a large-scale plant, as even a small increase in cost per unit area of the membrane spacer can impact the overall cost of the system. Thus, material selection and design optimization become crucial factors to be considered in a large-scale system. Aside from that, the study also concluded that a minimum of 10% improvement in water flux with no increase in pressure drop could economically justify the employment of a 3D-printed membrane spacer. Moreover, in a large-scale AGMD, even a moderate increment in flux water with steady or reduced pressure drop can exhibit a prominent COW reduction.

Nevertheless, many studies confirm that less fabrication expense is required through 3D printing as compared to conventional methods. One of the reasons is due to the additional costs associated with traditional manufacturing, such as the preparation of mold, dyes, finishing, additional tools, labor for assembly, and production unit costs of thousands of dollars [162]. For 3D printing, the costs that are taken into consideration are the 3D printer purchase cost (investment) and the materials used for the 3D printer [11]. Furthermore, it is reported that the cost of 3D printing equipment and the materials for the printing have decreased remarkably over a decade [163].

Further research regarding printing materials is greatly desired, as current materials often exhibit low tensile strength and reliability. This can be observed with the Polyjet 3D printing method, where the method itself is proven to be reliable in printing spacers. However, this method uses photo-curable resins that are heat and light-sensitive, which may degrade with time. Therefore, it is crucial to evaluate the polymer spacer produced for long-term utilization [155]. Despite its drawbacks, 3D printing technology remains beneficial in producing specialized products compared to conventional methods [14], which require significant capital investment.

More efforts should be devoted to enhancing water flux, lowering pressure drop in membrane modules, and increasing resistance toward fouling [22]. It is clear that the future development of membrane spacers remains promising, as reflected by recent research and publications, mainly focusing on modifying the materials of the spacer and the utilization of 3D printing technology. The application of 3D printing in spacer membranes and other areas holds vast potential and remarkable outcomes. In addition to being low-cost and flexible in creating various designs, with more discoveries from recent and future studies regarding potential materials, novel designs, and capabilities to reduce fouling, mainly biofouling, the future of 3D-printed spacers is encouraging. They have the potential to positively impact the future of water treatment industries.

5 Simulation of 3D printed spacer

Water and solute penetration within membrane modules, as well as the factors that govern membrane performance, have been subjects of experimental and theoretical study for decades to understand mass transfer phenomena in membrane processes. The most common form of module in large-scale RO plants is the spiral-wound membrane (SWM) module, which uses feed spacers to separate the membrane sheets, as shown in Fig. 16. By creating vortices near the membrane surfaces, feed spacers also encourage mixing, which can reduce CP and fouling at the expense of a higher pressure drop. To optimize the performance of an SWM module, it is crucial to understand how spacers affect the flow of mass and momentum. Designing efficient and effective NF and RO membrane processes relies heavily on optimizing momentum and mass transfer through feed spacer geometry [82,164−166].

While our understanding of mass transfer has been significantly advanced through experimental studies, our comprehension of the local and time-dependent phenomena occurring within membrane units remains limited. The study and identification of enhancement mechanisms are further complicated by the fact that conventional experimental methods tend to modify the flow field when making measurements close to the membrane wall. Computational methods may aid the study of mass transfer in membrane separation systems. Without affecting the flow itself, these methods can report on the state of the flow at any point in the geometry. In addition, numerical modeling dramatically diminishes the need for, and the cost of, repeated tests and experiments. CFD is a numerical method that can be used to assist in overcoming the limitations [166].

Understanding the hydrodynamic behavior of NF and RO membrane systems has become more feasible with the assistance of CFD [167]. Various types of feed channel spacers have been the subject of numerous CFD

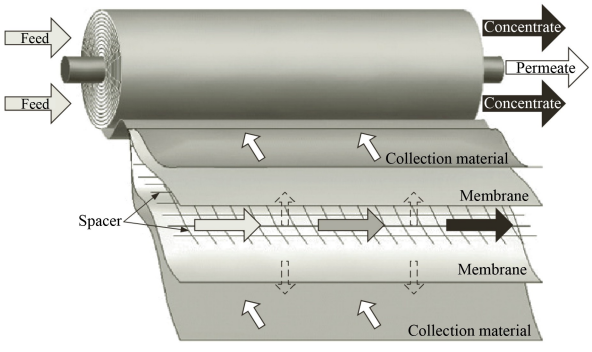

Fig. 16 A schematic of a spiral wound membrane module showing the flow directions, feed and permeate channels, including spacers. Reprinted with permission from Ref. [165], copyright 2008, Elsevier.

studies, examining their impact on fluid flow and mass transfer [168−171]. However, the majority of CFD research has focused on cylindrical structures, as it is possible to achieve numerical solution convergence with low-resolution meshing [167,171]. For non-cylindrical structures, such as those made possible by the advent of 3D printing technology aiming to improve mass transfer and reduce pressure loss, novel spacers like twisted spacers, multi-layer spacers, and perforated spacers can now be created with 3D printing [172]. There are fewer CFD and numerical studies for these non-cylindrical structures [171].

In modeling simulations, setting boundary conditions is crucial to outline the constraints of the systems and ensure they closely follow real-world operations. This boundary is defined by the region where the study's focus lies [173]. Selecting the boundary conditions is significant for predicting performance and outcomes such as permeate flux and fouling behavior. Most studies govern the incompressible continuity and Navier-Stokes equations for Newtonian fluids in channel flows within a spacer-filled membrane system [174,175]. Aside from that, in a spacer-filled channel, the flux of the membrane is highly influenced by the local trans-membrane pressure, driving force, and the effect of CP or fouling. Depending on the type of membrane system utilized in the modeling, suitable boundary conditions are required to support such a system. In some membrane systems, such as UF, osmotic pressure will rises due to the increased surface concentration, which leads to reduced flux. Since the accumulation of solutes at the membrane surface depends heavily on mass transfer, the boundary conditions to simulate the mass transfer must be suitably defined. Mass transfer can be described using the Sherwood correlation, which incorporates spacer geometry, diffusion coefficient, fluid viscosity, and cross-flow velocity [176]. In a study by El Kadi et al. [177], a simulation of a spacer-filled DCMD module was conducted. The flow was considered steady, and the boundary conditions defined for the system were the flow inlet as Dirichlet and the outlet as Neumann. The flow conditions applied included flow maintained in the laminar regime with an inlet velocity of 0.1 $m \cdot s^{-1}$, a feed inlet temperature of 75 °C, and a permeate inlet temperature of 25 °C. In addition, turbulence near the spacer was governed by the standard k-epsilon (k-ε) turbulent model. This section evaluates recent studies on 2D and 3D simulation and numerical analysis of feed spacers.

5.1 2D modeling of feed spacer membrane

Hydrodynamics and CP in spacer-filled membranes can be evaluated for energy usage optimization. Therefore, Ahmad et al. [178] integrated permeation properties into FLUENT 6 to explore how different spacer filaments affect unsteady hydrodynamics and CP in a spacer-filled membrane channel. A solute-solvent system was used for the feed, and the solute mass fraction was fixed at 0.005 kg solute per kg solution. The hydraulic permeability of the membrane was set at 4.72×10^{-11} $m \cdot Pa^{-1} \cdot s^{-1}$, and the reflection coefficient for the membrane was 0.98. Additionally, the transmembrane pressure was fixed at 11 bar, and the feed Reynolds number for the system was varied between 50 to 1200. The results of this modeling show that the transition length is shortest for a triangular spacer, followed by a cylinder, and finally a rectangle. Additionally, concentration factors generated by a cylindrical spacer are typically smaller than those generated by a rectangular spacer, provided that the operating Reynolds number is below 400. Therefore, a cylindrical spacer is preferable for use as a feed spacer in an SWM module. This also indicates that significant mass transfer improvement and reduction CP can result from interactions between forced transient flow and eddy inducers (i.e., spacers) in SWM modules. This led Foo et al. [170] to conduct a 2D CFD study on the effect of changing the geometric parameters of a 2D zig-zag spacer on the resonant frequency for an unstable forced slip and the subsequent permeate flux augmentation. This study utilized Navier-Stokes and mass transfer equations, the value of gravity is neglected, and laminar flow regimes are used (Re = 425). For spacer diameters in the center of the range examined ($0.5 < d_f/h_{ch} < 0.6$), an oscillating forced slip was found to be most successful at improving permeate flux.

2D CFD simulation can be helpful in illustrating mass transfer and pressure profiles. The effects of pressure losses, fluid flow patterns, and CP in open and spacer-filled channels were investigated using a finite element numerical model for three different configurations shown in Fig. 17 [179].

The movement of fluids in spacer-filled tubes can be obtained through Fig. 18, which shows the velocity vector

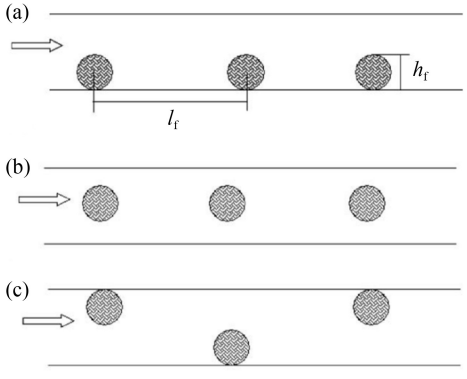

Fig. 17 Illustration of transverse spacer filament locations in straight-through CFMF channels with: (a) cavity, (b) submerged, and (c) zigzag spacer configurations. Flow is from left to right. Reprinted with permission from Ref. [179], copyright 2006, Elsevier.

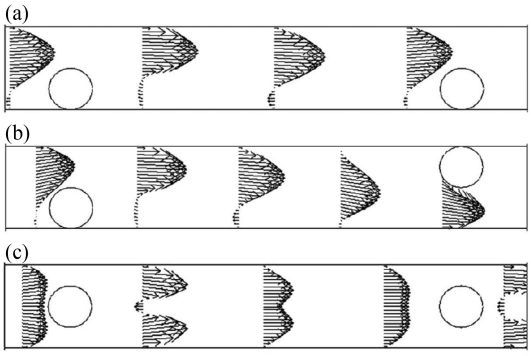

Fig. 18 Velocity vector diagrams for fluid flow through short sections of spacer-filled channels assuming: (a) cavity, (b) zigzag, and (c) submerged spacer configurations. Flow is from left to right. Reprinted with permission from Ref. [179], copyright 2006, Elsevier.

graphs. There is a flow reversal behind each filament in all three spacer designs, but the variations in size and intensity are significant. When the flow direction changes, eddies occur, leading to a local decrease in shear stress. As a result, the fluid flow patterns created by the various spacer configurations can either increase or decrease mass transfer and axial pressure losses in specific regions.

While 2D CFD models are computationally efficient and practically effective, they are incapable of representing the intricate geometric details of spacers, such as the intersection of filaments. Thus, 3D modeling has become valuable in this context.

5.2 3D modeling of feed spacer membrane

As mentioned earlier, due to certain limitations of 2D modeling and simulation, such as the inability to quantitatively evaluate the strand geometry of an asymmetrical spacer design concerning the main flow in a 2D setting [171], 3D modeling has become a valuable tool to overcome the issues. Another issue with 2D modeling is that it often accounts for equally spaced filaments of spherical, triangular, or square cross-sections [164,166,180]. Additionally, 2D numerical models do not consider the potential impact of axially oriented filaments parallel to the flow direction. Accurate descriptions of hydrodynamics, therefore, require the use of 3D simulations.

As a result, a novel 3D computational model was developed by Picioreanu et al. [180] that takes into account fluid dynamics, solute transport, and biofouling due to biofilm formation in NF and RO membrane modules. The model was applied to a computational domain consisting of 3 × 5 feed spacer frames with geometry representative of actual deployments. The researchers concluded that steady membrane installation performance at low costs might be significantly aided by the 3D mathematical modeling approach presented herein for biofouling of membrane modules.

In another study, spacer configuration efficacy (SCE) theory and other performance metrics were employed to evaluate a simple channel without any feed spacers and three additional channel topologies with feed spacers (a ladder, a triple, and a wavy or submerged configuration). Both membrane surfaces and all spacer filaments were treated as stationary, no-slip walls. The membranes were considered impermeable and non-porous, with a constant concentration boundary condition set at 35% w/w NaCl to simulate saturation conditions. The results showed that the mass transfer coefficient is significantly impacted by the estimated saturated solute concentration at the membrane. Among the obstructed geometries evaluated, the wavy spacer arrangement performed best based on SCE for $Re > 120$, while the Ladder-type geometry performed best for $Re \leqslant 120$ [181].

Another 3D modeling study by Chong et al. [172] focuses on RO SWM modules using ANSYS CFX 18.2, suggesting that they may benefit from spacer geometry changes. In this 3D CFD study, column and spherical nodes were used to analyze the hydrodynamic and mass transfer performance of submerged spacers with varying node shapes and sizes. In the simulation, the spacer filament was modeled as a no-slip wall with zero mass flux, while the membrane surfaces were considered impermeable, dissolving boundaries with a constant solute concentration. The feed inlet velocity was set at 0.03 to 0.17 $m \cdot s^{-1}$, and the transmembrane pressure was 6.5 MPa. As shown in Fig. 19, the Sherwood number and wall shear both rise by 25% at the expense of a greater global friction factor (44%) when the dimensionless node diameter ratio of the column nodes is increased from 0.3 to 1.2. Since the mixing effects of the spacer that promote mass transfer are more noticeable at high feed inlet velocity (> 0.1 $m \cdot s^{-1}$), a full-scale examination of seawater RO found that column node spacers yield higher average flux than spherical nodes and conventional spacers.

6 Conclusions

In this study, the advancements of membrane spacers through the modification of geometric design, materials, 3D printing methods, and simulations have been discussed, highlighting the high potential for the future of membrane spacers. Regarding the modification of spacers through geometric design, it is observed that the shape, thickness, and even the length of the design impact the overall performance of the spacer. Currently, the most optimal design for a membrane spacer is an optimal multi-layer spacer with optimal non-woven nets in the outer layers and twisted tapes in the middle layer. Several studies indicate that the thickest spacer provides the best

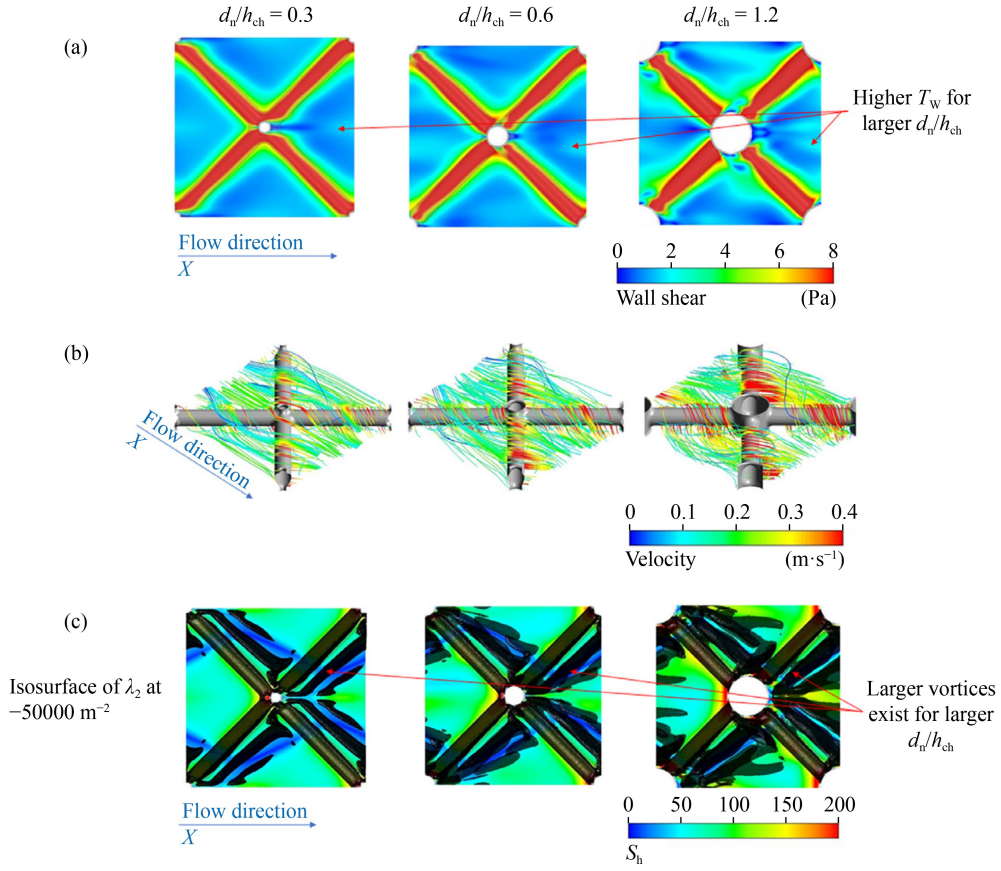

Fig. 19 (a) Surface profile of τw, (b) streamline plot, (c) iso surface plots of regions with –50000 m^{-2} λ_2 and surface profile of S_h for different d_n/h_{ch} column nodes spacers at Re_h = 200 [172], copyright 2022, Elsevier.

performance with minimal effects on biofouling and flux decline. However, one study showed that a very thin spacer provides better performance, contradicting some previous studies. This issue needs further investigation, exploring the performance differences between thin spacers and thick spacers. Additionally, a non-woven spacer with a mesh angle of 60° demonstrates the best performance, but there is limited research on the mesh angle of membrane spacers. More studies are focusing on fabricating novel geometric designs and are yielding exciting results that can be used as references in the future.

This study also provides insights into the modification of membrane spacers through material innovation, where experimentation with different materials focuses on fluid flow characteristics and reducing biofouling. Previous studies on these issues have led to a range of innovative approaches to enhance spacer efficiency. For example, metallic spacers fabricated from high thermal conductivity materials such as copper and nickel have been proven to increase the efficiency of thermally driven processes, such as membrane distillation. Numerous studies have also experimented with coating spacers with various materials or mixing spacer materials with other nanomaterials to reduce biofouling. With the rise of 3D printing in the membrane technology field, the array of materials available for spacers has expanded, each offering unique finishes and performance characteristics. Additionally, the blending of nanomaterials with 3D printing materials remains underexplored, and the possibilities are promising. Regarding the application of 3D-printed spacers in large-scale applications, there are various limitations that are still being studied, including limitations with mass production, time-consuming manufacturing, materials degradation, cost, and limited long-term performance knowledge. Although 3D-printed spacers exhibited enhanced properties due to design optimization, the high material costs contribute significantly to CAPEX. However, design optimization that lowers pressure drop (reduces pumping energy) and increases water flux (decreases thermal energy) offers potential reduction in OPEX. These performances may offset the initial higher cost in long-term operation, mainly in thermally driven membrane processes such as membrane distillation.

Since the 3D printing method is currently an area of active research for membrane spacers, this study also provides insights into the utilization of 3D printing methods to fabricate membrane spacers. This topic is fascinating, and more profound research and discussions are foreseen in the future. Currently, the selection of a 3D printing method is based on the desired finishing features

of the membrane spacer, given the various 3D printing methods available, each with its pros and cons to consider. With the assistance of 3D simulations, research on membrane spacers has become more convenient, particularly in the study of fluid dynamics, solute transport, and biofouling due to biofilm formation. Since the modification of membrane spacers leaves ample space for exploration, especially with the implementation of 3D printing methods, it is sensible that studies on the modification of membrane spacers are still progressively conducted, and the need for further study is encouraged.

7 Future prospectives

Despite numerous research efforts on alternatives to decrease biofouling through geometric and material modifications, this issue remains a challenge. Studies on fabricating novel designs that could decrease dead zones of the membrane spacer, and studies on incorporating nanomaterials in 3D print materials, are increasing significantly as there are many possibilities that exist to increase the efficiency of the membrane. In addition to implementing 3D printing methods to fabricate the membrane spacers, blending materials and testing other designs are robust alternatives to produce a highly efficient spacer. As biofouling remains a significant issue in membrane filtration systems, utilizing antimicrobial materials such as silver is an excellent idea. Furthermore, adding other materials, such as graphene oxide, to enhance the strength of the membrane spacer and act as a medium for the uniform distribution of antimicrobial materials on the membrane is another viable approach. With the convenience that 3D printing methods provide, more designs need to be studied, as the possibilities are endless, and they may open new directions to another branch of study in the membrane spacer field.

Competing interests The authors declare that they have no competing interests.

Acknowledgements The authors would like to acknowledge the funding provided by the Ministry of Higher Education Malaysia through the Fundamental Research Grant Scheme (FRGS/1/2021/TK0/UKM/02/41).

Funding Note Open access funding provided by the Ministry of Higher Education Malaysia and Oniversiti Kebangsaan Malaysia.

References

1. Khalil A, Ahmed F E, Hilal N. The emerging role of 3D printing in water desalination. Science of the Total Environment, 2021, 790: 148238
2. Lee M, Keller A A, Chiang P C, Den W, Wang H, Hou C H, Wu J, Wang X, Yan J. Water-energy nexus for urban water systems: a comparative review on energy intensity and environmental impacts in relation to global water risks. Applied Energy, 2017, 205: 589–601
3. Banerjee P, Das R, Das P, Mukhopadhyay A. Membrane technology. Carbon Nanostructures, Berlin: Springer, 2018, 127–150
4. Haddad A. Coping with water scarcity. Water and Wastewater International, 2007, 22(3): 1–10
5. Madhura L, Kanchi S, Sabela M I, Singh S, Bisetty K, Inamuddin. Membrane technology for water purification. Environmental Chemistry Letters, 2018, 16(2): 343–365
6. Rahmawati R, Bilad M R, Nawi N I M, Wibisono Y, Suhaimi H, Shamsuddin N, Arahman N. Engineered spacers for fouling mitigation in pressure driven membrane processes: progress and projection. Journal of Environmental Chemical Engineering, 2021, 9(5): 106285
7. Kamali M, Suhas D P, Costa M E, Capela I, Aminabhavi T M. Sustainability considerations in membrane-based technologies for industrial effluents treatment. Chemical Engineering Journal, 2019, 368: 474–494
8. Goh P S, Ismail A F. A review on inorganic membranes for desalination and wastewater treatment. Desalination, 2018, 434(7): 60–80
9. Pan Z, Song C, Li L, Wang H, Pan Y, Wang C, Li J, Wang T, Feng X. Membrane technology coupled with electrochemical advanced oxidation processes for organic wastewater treatment: recent advances and future prospects. Chemical Engineering Journal, 2019, 376: 120909
10. Ying Y, Ying W, Li Q, Meng D, Ren G, Yan R, Peng X. Recent advances of nanomaterial-based membrane for water purification. Applied Materials Today, 2017, 7: 144–158
11. Thiam B G, El Magri A, Vanaei H R, Vaudreuil S. 3D printed and conventional membranes: a review. Polymers, 2022, 14(5): 1023
12. Xie M, Shon H K, Gray S R, Elimelech M. Membrane-based processes for wastewater nutrient recovery: technology, challenges, and future direction. Water Research, 2016, 89: 210–221
13. Lin W, Zhang Y, Li D, Wang X, Huang X. Roles and performance enhancement of feed spacer in spiral wound membrane modules for water treatment: a 20-year review on research evolvement. Water Research, 2021, 198: 117146
14. Ng V H, Koo C H, Chong W C, Tey J Y. Progress of 3D printed feed spacers for membrane filtration. Materials Today: Proceedings, 2021, 46(5): 2070–2077

15. Park H G, Cho S G, Kim K J, Kwon Y N. Effect of feed spacer thickness on the fouling behavior in reverse osmosis process: a pilot scale study. Desalination, 2016, 379: 155–163
16. Jeong K, Park M, Oh S, Ha J. Impacts of flow channel geometry, hydrodynamic, and membrane properties on osmotic backwash of RO membranes—CFD modeling and simulation. Desalination, 2020, 476: 114229
17. Luo J, Li M, Heng Y. A hybrid modeling approach for optimal design of non-woven membrane channels in brackish water reverse osmosis process with high-throughput computation. Desalination, 2020, 489: 114463
18. Siebdrath N, Farhat N, Ding W, Kruithof J, Johannes S. Impact of membrane biofouling in the sequential development of performance indicators: feed channel pressure drop, permeability, and salt rejection. Journal of Membrane Science, 2019, 585: 199–207
19. Kerdi S, Qamar A, Vrouwenvelder J S, Ghaffour N. Fouling resilient perforated feed spacers for membrane filtration. Water Research, 2018, 140: 211–219
20. Ruiz-garcía A, Nuez I. Feed spacer geometries and permeability coefficients: effect on the performance in BWRO spriral-wound membrane modules. Water, 2019, 11(1): 152
21. Koo J W, Ho J S, An J, Zhang Y, Chua C K, Chong T H. A review on spacers and membranes: conventional or hybrid additive manufacturing? Water Research, 2021, 188: 116497
22. Abid H S, Johnson D J, Hashaikeh R, Hilal N. A review of efforts to reduce membrane fouling by control of feed spacer characteristics. Desalination, 2017, 420: 384–402
23. Qian X, Anvari A, Hoek E M V, Mccutcheon J R. Advancements in conventional and 3D printed feed spacers in membrane modules. Desalination, 2023, 556: 116518
24. Ali S M, Kim Y, Qamar A, Gayathri N, Phuntsho S, Noreddine G, Vrouwenvelder J S, Shon H K. Dynamic feed spacer for fouling minimization in forward osmosis process. Desalination, 2021, 515: 115198
25. Siddiqui A, Lehmann S, Bucs S S, Fresquet M, Fel L, Prest E I E C, Ogier J, Schellenberg C, van Loosdrecht M C M, Kruithof J C, et al. Predicting the impact of feed spacer modification on biofouling by hydraulic characterization and biofouling studies in membrane fouling simulators. Water Research, 2017, 110: 281–287
26. Park C, Kim J O. Performance of biofouling mitigating feed spacer by surface modification using quorum sensing inhibitor. Desalination, 2022, 538: 115904
27. Ng C Y, Mohammad A W, Ng L Y, Jahim J M. Membrane fouling mechanisms during ultrafiltration of skimmed coconut milk. Journal of Food Engineering, 2014, 142: 190–200
28. Choudhury M R, Anwar N, Jassby D, Rahaman M S. Fouling and wetting in the membrane distillation driven wastewater reclamation process: a review. Advances in Colloid and Interface Science, 2019, 269: 370–399
29. Alkhatib A, Ayari M A, Hawari A H. Fouling mitigation strategies for different foulants in membrane distillation. Chemical Engineering and Processing, 2021, 167: 108517
30. Piyadasa C, Ridgway H F, Yeager T R, Stewart M B, Pelekani C, Gray S R, Orbell J D. The application of electromagnetic fields to the control of the scaling and biofouling of reverse osmosis membranes: a review. Desalination, 2017, 418: 19–34
31. Goh P S, Lau W J, Othman M H D, Ismail A F. Membrane fouling in desalination and its mitigation strategies. Desalination, 2018, 425: 130–155
32. Liu L, Xiao Z, Liu Y, Li X, Yin H, Volkov A, He T. Understanding the fouling/scaling resistance of superhydrophobic/omniphobic membranes in membrane distillation. Desalination, 2021, 499: 114864
33. Ahmed M A, Amin S, Mohamed A A. Fouling in reverse osmosis membranes: monitoring, characterization, mitigation strategies, and future directions. Heliyon, 2023, 9(4): e14908
34. Tang C Y, Chong T H, Fane A G. Colloidal interactions and fouling of NF and RO membranes: a review. Advances in Colloid and Interface Science, 2011, 164(1–2): 126–143
35. Adel M, Nada T, Amin S, Anwar T, Mohamed A A. Characterization of fouling for a full-scale seawater reverse osmosis plant on the Mediterranean sea: membrane autopsy and chemical cleaning efficiency. Groundwater for Sustainable Development, 2022, 16: 100704
36. Yang H, Ye S, Wang J, Wang H, Wang Z, Chen Q, Wang W, Xiang L, Zeng G, Tan X. The approaches and prospects for natural organic matter-derived disinfection byproducts control by carbon-based materials in water disinfection progresses. Journal of Cleaner Production, 2021, 311: 127799
37. Cai Y H, Galili N, Gelman Y, Herzberg M, Gilron J. Evaluating the impact of pretreatment processes on fouling of reverse osmosis membrane by secondary wastewater. Journal of Membrane Science, 2021, 623: 119054
38. Ly Q V, Hu Y, Li J, Cho J, Hur J. Characteristics and influencing factors of organic fouling in forward osmosis operation for wastewater applications: a comprehensive review. Environment International, 2019, 129: 164–184
39. Di Martino P. Extracellular polymeric substances, a key element in understanding biofilm phenotype. AIMS Microbiology, 2018, 4(2): 274–288
40. Flemming H C, Schaule G, McDonogh R, Ridgway H F. Biofouling and Biocorrosion in Industrial Water Systems. Boca Raton: CRC Press, 1994, 63–105
41. Baker J, Stephenson T, Dard S, Côté P. Characterisation of fouling of nanofiltration membranes used to treat surface waters. Environmental Technology, 1995, 16(10): 977–985
42. Van Paassen J A M, Kruithoi J C, Bakker S M, Kegel F S. Integrated multi-objective membrane systems for surface water treatment: pre-treatment of nanofiltration by riverbank filtration and conventional ground water treatment. Desalination, 1998, 118(1–3): 239–248
43. Ridgway H F. Membrane biofouling: an international workshop. National Water Research Institute Occasional Paper Number NWRI-97–3, 1997
44. Sreedhar N, Thomas N, Ghaffour N, Arafat H A. The evolution of feed spacer role in membrane applications for desalination and water treatment: a critical review and future perspective. Desalination, 2023, 554: 116505
45. Kleinstreuer C. Modern Fluid Dynamics. Dordrecht: Springer, 2006, 2–3

46. Ella H AE. AERO 4304: Computational Fluid Dynamics—Course Outline. Carleton University website
47. Vrouwenvelder J S, Graf von der Schulenburg D A, Kruithof J C, Johns M L, van Loosdrecht M C M. Biofouling of spiral-wound nanofiltration and reverse osmosis membranes: a feed spacer problem. Water Research, 2009, 43(3): 583–594
48. Vrouwenvelder J S, van Paassen J A M, van Agtmaal J M C, van Loosdrecht M C M, Kruithof J C. A critical flux to avoid biofouling of spiral wound nanofiltration and reverse osmosis membranes: fact or fiction? Journal of Membrane Science, 2009, 326(1): 36–44
49. de Vries H J, Kleibusch E, Hermes G D A, van den Brink P, Plugge C M. Biofouling control: the impact of biofilm dispersal and membrane flushing. Water Research, 2021, 198: 117163
50. Flemming H C. Biofouling in water systems—cases, causes, and countermeasures. Applied Microbiology and Biotechnology, 2002, 59(6): 629–640
51. Bucs S S, Farhat N, Kruithof J C, Picioreanu C, Van Loosdrecht M C M, Vrouwenvelder J S. Review on strategies for biofouling mitigation in spiral wound membrane systems. Desalination, 2018, 434: 189–197
52. Kerdi S, Qamar A, Vrouwenvelder J S, Ghaffour N. Effect of localized hydrodynamics on biofilm attachment and growth in a cross-flow filtration channel. Water Research, 2021, 188: 116502
53. AlSawaftah N, Abuwatfa W, Darwish N, Husseini G A. A review on membrane biofouling: prediction, characterization, and mitigation. Membranes, 2022, 12(12): 1271
54. Nguyen T, Roddick F A, Fan L. Biofouling of water treatment membranes: a review of the underlying causes, monitoring techniques, and control measures. Membranes, 2012, 2(4): 804–840
55. Jiang S, Li Y, Ladewig B P. A review of reverse osmosis membrane fouling and control strategies. Science of the Total Environment, 2017, 595: 567–583
56. Chua S F, Nouri A, Ang W L, Mahmoudi E, Mohammad A W, Benamor A, Ba-Abbad M. The emergence of multifunctional adsorbents and their role in environmental remediation. Journal of Environmental Chemical Engineering, 2021, 9(1): 104793
57. Syron E, Semmens M J, Casey E. Performance analysis of a pilot-scale membrane aerated biofilm reactor for the treatment of landfill leachate. Chemical Engineering Journal, 2015, 273: 120–129
58. Zare S, Kargari A. Membrane properties in membrane distillation. Emerging Technologies for Sustainable Desalination Handbook, 2018: 107–156
59. Lin W C, Shao R P, Wang X M, Huang X. Impacts of non-uniform filament feed spacers characteristics on the hydraulic and anti-fouling performances in the spacer-filled membrane channels: experiment and numerical simulation. Water Research, 2020, 185: 116251
60. Briand J F. Marine antifouling laboratory bioassays: an overview of their diversity. Biofouling, 2009, 25(4): 297–311
61. Chua S F, Nouri A, Mahmoudi E, Lun W. Modified-graphene quantum dot thin-film nanocomposite membrane for enhanced nanofiltration performance and antifouling properties: minimal incorporation. Journal of Water Process Engineering, 2023, 53: 103664
62. Mukherjee M, Bandyopadhyaya R. Silver nanoparticle impregnated polyethersulfone ultrafiltration membrane: optimization of degree of grafting of acrylic acid for biofouling prevention and improved water permeability. Journal of Environmental Chemical Engineering, 2020, 8(2): 103711
63. Ng L Y, Chua H S, Ng C Y. Incorporation of graphene oxide-based nanocomposite in the polymeric membrane for water and wastewater treatment: a review on recent development. Journal of Environmental Chemical Engineering, 2021, 9(5): 105994
64. Ng V H, Koo C H, Chong W C, Tey J Y. Progress of 3D printed feed spacers for membrane filtration. Materials Today: Proceedings, 2020, 46(5): 2070–2077
65. Lin W, Li D, Wang Q, Wang X M, Huang X. Dynamic evolution of membrane biofouling in feed channels 2 affected by spacer-membrane clearance and the induced 3 hydrodynamic conditions. Journal of Membrane Science, 2023, 668: 121209
66. Løge I A, Bentzon J R, Klingaa C G, Walther J H, Anabaraonye B U, Fosbøl P L. Scale attachment and detachment: the role of hydrodynamics and surface morphology. Chemical Engineering Journal, 2022, 430(2): 132583
67. Jiang B, Hu B, Yang N, Zhang L, Sun Y, Xiao X. Study of turbulence promoters in prolonging membrane life. Membranes, 2021, 11(4): 268
68. Al-Amshawee S K A, Mohd Yunus M Y B. Impact of membrane spacers on concentration polarization, flow profile, and fouling at ion exchange membranes of electrodialysis desalination: diagonal net spacer *vs*. ladder-type configuration. Chemical Engineering Research & Design, 2023, 191: 197–213
69. Bhattacharjee C, Saxena V K, Dutta S. Static turbulence promoters in cross-flow membrane filtration: a review. Chemical Engineering Communications, 2020, 207(3): 413–433
70. Zamani F, Chew J W, Akhondi E, Krantz W B, Fane A G. Unsteady-state shear strategies to enhance mass-transfer for the implementation of ultrapermeable membranes in reverse osmosis: a review. Desalination, 2015, 356: 328–348
71. Awais M, Bhuiyan A A. Recent advancements in impedance of fouling resistance and particulate depositions in heat exchangers. International Journal of Heat and Mass Transfer, 2019, 141: 580–603
72. Du X, Wang Y, Leslie G, Li G, Liang H. Shear stress in a pressure-driven membrane system and its impact on membrane fouling from a hydrodynamic condition perspective: a review. Journal of Chemical Technology and Biotechnology, 2017, 92(3): 463–478
73. Wray H E, Andrews R C, Bérubé P R. Surface shear stress and membrane fouling when considering natural water matrices. Desalination, 2013, 330: 22–27
74. Koutsou C P, Yiantsios S G, Karabelas A J. A numerical and experimental study of mass transfer in spacer-filled channels: effects of spacer geometrical characteristics and Schmidt number. Journal of Membrane Science, 2009, 326(1): 234–251
75. Kerdi S, Qamar A, Tanudjaja H J, Ghaffour N. Spacer designs for improved hydrodynamics and filtration efficiency in sea water reverse osmosis. Membranes, 2025, 15(1): 32

76. Dendukuri D, Karode S K, Kumar A. Flow visualization through spacer filled channels by computational fluid dynamics-II: improved feed spacer designs. Journal of Membrane Science, 2005, 249(1–2): 41–49
77. Armbruster S, Stockmeier F, Junker M, Schiller-Becerra M, Yüce S, Wessling M. Short and spaced twisted tapes to mitigate fouling in tubular membranes. Journal of Membrane Science, 2020, 595: 117426
78. Ibrahim A A, Dalle M A, Janasz F, Leyer S. Novel spacer geometries for membrane distillation mixing enhancement. Desalination, 2024, 580: 117513
79. Yanar N, Liang Y, Yang E, Park H, Son M, Choi H. Electrically polarized graphene-blended spacers for organic fouling reduction in forward osmosis. Membranes, 2021, 11(1): 36
80. Al-Obaidi M A, Rashid F L, Ameen A, Kadhom M, Mujtaba I M. Optimizing reverse osmosis feed spacer design for enhanced dimethylphenol removal from wastewater: a study of hydrodynamics and performance indicators. Water, 2024, 16(6): 895
81. Joshi S R, Ray S S, Kim S, Kwon Y N. Potentiality of PLA 3D printed macro-structured feed spacers with a rational and facile layout for improved MD desalination performance. Chemical Engineering Research & Design, 2024, 203: 293–304
82. Gu B, Adjiman C S, Xu X Y. The effect of feed spacer geometry on membrane performance and concentration polarisation based on 3D CFD simulations. Journal of Membrane Science, 2016, 2017(527): 78–91
83. Marsono B D, Agustina I, Yuniarto A, Hermana J. Pressure and spacer effect on the performance of immersed microfiltration membrane. IOP Conference Series: Earth and Environmental Science, 2022, 1111(1): 012063
84. Mehdizadeh S, Yasukawa M, Abo T, Kakihana Y, Higa M. Effect of spacer geometry on membrane and solution compartment resistances in reverse electrodialysis. Journal of Membrane Science, 2019, 572: 271–280
85. Li F, Meindersma W, De Haan A B, Reith T. Novel spacers for mass transfer enhancement in membrane separations. Journal of Membrane Science, 2005, 253(1–2): 1–12
86. Mahdieh H A, Talebbeydokhti N, Afzali S H, Karimi-Jashni A. Development and evaluation of a novel feed spacer for forward osmosis membrane. Process Safety and Environmental Protection, 2022, 159: 874–886
87. Ali S M, Qamar A, Kerdi S, Phuntsho S, Vrouwenvelder J S, Ghaffour N, Shon H K. Energy efficient 3D printed column type feed spacer for membrane filtration. Water Research, 2019, 164: 114961
88. Kerdi S, Qamar A, Alpatova A, Vrouwenvelder J S, Ghaffour N. Membrane filtration performance enhancement and biofouling mitigation using symmetric spacers with helical filaments. Desalination, 2020, 484: 114454
89. Qamar A, Kerdi S, Ali S M, Shon H K, Vrouwenvelder J S, Ghaffour N. Novel hole-pillar spacer design for improved hydrodynamics and biofouling mitigation in membrane filtration. Scientific Reports, 2021, 11(1): 6979
90. AlQattan J, Kim Y, Kerdi S, Qamar A, Ghaffour N. Hole-type spacers for more stable shale gas-produced water treatment by forward osmosis. Membranes, 2021, 11(1): 34
91. Park S, Jeong Y D, Lee J H, Kim J, Jeong K, Cho K H. 3D printed honeycomb-shaped feed channel spacer for membrane fouling mitigation in nanofiltration. Journal of Membrane Science, 2021, 620: 118665
92. Tan Y Z, Ang E H, Chew J W. Metallic spacers to enhance membrane distillation. Journal of Membrane Science, 2018, 2019(572): 171–183
93. Thamaraiselvan C, Carmiel Y, Eliad G, Sukenik C N, Semiat R, Dosoretz C G. Modification of a polypropylene feed spacer with metal oxide-thin film by chemical bath deposition for biofouling control in membrane filtration. Journal of Membrane Science, 2019, 573: 511–519
94. Thamaraiselvan C, Manderfeld E, Rosenhahn A, Arnusch C J. Superhydrophobic candle soot as a low fouling stable coating on water treatment membrane feed spacers. ACS Applied Bio Materials, 2021, 4(5): 4191–4200
95. Taiswa A, Andriolo J M, Zodrow K R, Skinner J L. Polydopamine-copper spacers improve longevity and prevent biofouling in reverse osmosis. Water Science and Technology: Water Supply, 2022, 22(10): 7782–7793
96. Tan J X, Foo K, Lau W J, Chua S F, Rahim M H A, Ahmad A L, Liang Y Y. Hydrophilic modification of feed spacer and its impacts on antifouling performance of reverse osmosis membrane. Asia-Pacific Journal of Chemical Engineering, 2024, 19(6): e3134
97. Ronen A, Semiat R, Dosoretz C G. Impact of ZnO embedded feed spacer on biofilm development in membrane systems. Water Research, 2013, 47(17): 6628–6638
98. Ronen A, Lerman S, Ramon G Z, Dosoretz C G. Experimental characterization and numerical simulation of the anti-biofuling activity of nanosilver-modified feed spacers in membrane filtration. Journal of Membrane Science, 2015, 475: 320–329
99. Wibisono Y, Yandi W, Golabi M, Nugraha R, Cornelissen E R, Kemperman A J B, Ederth T, Nijmeijer K. Hydrogel-coated feed spacers in two-phase flow cleaning in spiral wound membrane elements: anovel platform for eco-friendly biofouling mitigation. Water Research, 2015, 71: 171–186
100. Ronen A, Resnick A, Lerman S, Eisen M S, Dosoretz C G. Biofouling suppression of modified feed spacers: localized and long-distance antibacterial activity. Desalination, 2016, 393: 159–165
101. Jab M, Menzel M, Hirsch U, Heilmann A. Assessment of anti-bacterial adhesion and anti-biofouling potential of plasma-mediated poly(sulfobetaine methacrylate) coatings of feed spacer. Desalination, 2020, 493(4): 114664
102. Pisharody L, Thamaraiselvan C, Manderfeld E, Singh S P, Rosenhahn A, Arnusch C J. Antimicrobial and antibiofouling electrically conducting laser-induced graphene spacers in reverse osmosis membrane modules. Advanced Materials Interfaces, 2022, 9(33): 2201443
103. Kitano H, Takeuchi K, Ortiz-medina J, Cruz-silva R, Morelos-gomez A, Fujii M, Obata M, Yamanaka A, Tejima S, Fujishige M, et al. Enhanced antifouling feed spacer made from a carbon nanotube-polypropylene nanocomposite. ACS Omega, 2019, 4(13): 15496–15503

104. Ibrahim Y, Hilal N. The potentials of 3D-printed feed spacers in reducing the environmental footprint of membrane separation processes. Journal of Environmental Chemical Engineering, 2023, 11(1): 109249
105. Yanar N, Son M, Yang E, Kim Y, Park H, Nam S E, Choi H. Investigation of the performance behavior of a forward osmosis membrane system using various feed spacer materials fabricated by 3D printing technique. Chemosphere, 2018, 202: 708–715
106. Yanar N, Park H, Son M, Choi H. Efficacy of electrically-polarized 3D printed graphene-blended spacers on the flux enhancement and scaling resistance of water filtration membranes. ACS Sustainable Chemistry & Engineering, 2021, 9(19): 6623–6631
107. Ibrahim Y, Hilal N. Integration of porous and permeable poly(ether sulfone) feed spacer onto membrane surfaces via direct 3D printing. ACS Applied Engineering Materials, 2024, 2(4): 1094–1109
108. Thomas N, Sreedhar N, Al-Ketan O, Rowshan R, Abu Al-Rub R K, Arafat H. 3D printed spacers based on TPMS architectures for scaling control in membrane distillation. Journal of Membrane Science, 2019, 581: 38–49
109. Castillo E H C, Thomas N, Al-Ketan O, Rowshan R, Abu Al-Rub R K, Nghiem L D, Vigneswaran S, Arafat H A, Naidu G. 3D printed spacers for organic fouling mitigation in membrane distillation. Journal of Membrane Science, 2019, 581: 331–343
110. Sreedhar N, Thomas N, Al-Ketan O, Rowshan R, Abu Al-Rub R K, Hong S, Arafat H A. Impacts of feed spacer design on UF membrane cleaning efficiency. Journal of Membrane Science, 2020, 616: 118571
111. Wee J, Shin J, Zen Y, See W, An J, Zhang Y, Kai C, Haur T. Fouling mitigation in reverse osmosis processes with 3D printed sinusoidal spacers. Water Research, 2021, 207: 117818
112. Dang B Van, Charlton A J, Li Q, Kim Y C, Taylor R A, Le-Clech P, Barber T. Can 3D-printed spacers improve filtration at the microscale? Separation and Purification Technoly, 2021, 256: 117776
113. Thomas N, Kumar M, Palmisano G, Al-rub R K A, Alnuaimi R Y, Alhseinat E, Rowshan R, Arafat H A, Platforms C T, York N, et al. Antiscaling 3D printed feed spacers via facile nanoparticle coating for membrane distillation. Water Research, 2021, 189: 116649
114. Thomas N, Swaminathan J, Zaragoza G, Abu Al-Rub R K, Lienhard V J H, Arafat H A. Comparative assessment of the effects of 3D printed feed spacers on process performance in MD systems. Desalination, 2021, 503: 114940
115. Khalil A, Ahmed F E, Hashaikeh R, Hilal N. 3D printed electrically conductive interdigitated spacer on ultrafiltration membrane for electrolytic cleaning and chlorination. Journal of Applied Polymer Science, 2022, 139(23): 52292
116. Yu J, Chen D, Wu J J, Wang B, Field R W. Arch-type feed spacer with wide passage node design for spiral-wound membrane filtration with reduced energy cost. Desalination, 2022, 540: 115980
117. Suresh K, Nambikkattu J, Kaleekkal N J, Lawrence K D. Custom-designed 3D printed feed spacers and TFN membranes with MIL-101(Fe) for water recovery by forward osmosis. Environmental Technology, 2024, 45(19): 3778–3790
118. Almarzooqi N, Hong S, Verma P, Shaheen A, Schiffer A, AlMarzooqi F. Photothermal surface heating membrane distillation using 3D-printed $Ti_3C_2T_x$ MXene-based nanocomposite spacers. ACS Applied Materials & Interfaces, 2023, 15(17): 20998–21007
119. Jeong S, Gu B, Choi S, Ahn S kyun, Lee J, Lee J, Jeong S. Engineered multi-scale roughness of carbon nanofiller-embedded 3D printed spacers for membrane distillation. Water Research, 2023, 231: 119649
120. Qamar A, Kerdi S, Vrouwenvelder J S, Ghaffour N. Airfoil-shaped filament feed spacer for improved filtration performance in water treatment. Scientific Reports, 2023, 13(1): 10798
121. Lv Y, Du Y, Qiu W Z, Xu Z K. Nanocomposite membranes via the codeposition of polydopamine/polyethylenimine with silica nanoparticles for enhanced mechanical strength and high water permeability. ACS Applied Materials & Interfaces, 2017, 9(3): 2966–2972
122. Coakley M, Hurt D E. 3D printing in the laboratory: maximize time and funds with customized and open-source labware. SLAS Technology, 2016, 21(4): 489–495
123. Awad A, Fina F, Goyanes A, Gaisford S, Basit A W. 3D printing: principles and pharmaceutical applications of selective laser sintering. International Journal of Pharmaceutics, 2020, 586: 119594
124. Zhuang Y, Guo Y, Li J, Jiang K, Zhang H, Meng D. Study on process and parameter optimisation of selective laser sintering of thermoplastic polyurethane/carbon nanotube powder. International Journal of Advanced Manufacturing Technology, 2021, 116(3–4): 993–1001
125. Campbell C G, Astorga D J, Martinez E, Celina M. Selective laser sintering (SLS)-printable thermosetting resins via controlled conversion. MRS Communications, 2021, 11(2): 173–178
126. Yuan S, Strobbe D, Kruth J P, Van Puyvelde P, Van der Bruggen B. Production of polyamide-12 membranes for microfiltration through selective laser sintering. Journal of Membrane Science, 2017, 525: 157–162
127. Tan W S, Chua C K, Chong T H, Fane A G, Jia A. 3D printing by selective laser sintering of polypropylene feed channel spacers for spiral wound membrane modules for the water industry. Virtual and Physical Prototyping, 2016, 11(3): 151–158
128. Yang F, Zobeiry N, Mamidala R, Chen X. A review of aging, degradation, and reusability of PA12 powders in selective laser sintering additive manufacturing. Materials Today: Communications, 2023, 34: 105279
129. Al-Shimmery A, Mazinani S, Ji J, Chew Y M J, Mattia D. 3D printed composite membranes with enhanced anti-fouling behaviour. Journal of Membrane Science, 2018, 2019(574): 76–85
130. Yuan S, Strobbe D, Li X, Kruth J P, van Puyvelde P, van der Bruggen B. 3D printed chemically and mechanically robust membrane by selective laser sintering for separation of oil/water and immiscible organic mixtures. Chemical Engineering Journal, 2020, 385: 123816

131. Sun P, Zhang L, Tao S. Preparation of hybrid chitosan membranes by selective laser sintering for adsorption and catalysis. Materials & Design, 2019, 173: 107780
132. Xu Y, Wu X, Guo X, Kong B, Zhang M, Qian X, Mi S, Sun W. The boom in 3D-printed sensor technology. Sensors, 2017, 17(5): 1166
133. Kim S G, Song J E, Kim H R. Development of fabrics by digital light processing three-dimensional printing technology and using a polyurethane acrylate photopolymer. Textile Research Journal, 2020, 90(7–8): 847–856
134. Riahi M. Fabrication of corner cube array retro-reflective structure with DLP-based 3D printing technology. Optical Review, 2016, 23(3): 442–447
135. Monzón M, Ortega Z, Hernández A, Paz R, Ortega F. Anisotropy of photopolymer parts made by digital light processing. Materials, 2017, 10(1): 64
136. Chen T, Wang D, Chen X, Qiu M, Fan Y. Three-dimensional printing of high-flux ceramic membranes with an asymmetric structure via digital light processing. Ceramics International, 2022, 48(1): 304–312
137. Udroiu R, Braga I C. Polyjet technology applications for rapid tooling. MATEC Web of Conferences, 2017, 112: 1–6
138. Lee J Y, Tan W S, An J, Chua C K, Tang C Y, Fane A G, Chong T H. The potential to enhance membrane module design with 3D printing technology. Journal of Membrane Science, 2016, 499: 480–490
139. Siddiqui A, Farhat N, Bucs S S, Linares R V, Picioreanu C, Kruithof J C, van Loosdrecht M C M, Kidwell J, Vrouwenvelder J S. Development and characterization of 3D-printed feed spacers for spiral wound membrane systems. Water Research, 2016, 91: 55–67
140. Yanar N, Son M, Park H, Choi H. Bio-mimetically inspired 3D-printed honeycombed support (spacer) for the reduction of reverse solute flux and fouling of osmotic energy driven membranes. Journal of Industrial and Engineering Chemistry, 2020, 83: 343–350
141. Tan W S, Suwarno S R, An J, Chua C K, Fane A G, Chong T H. Comparison of solid, liquid and powder forms of 3D printing techniques in membrane spacer fabrication. Journal of Membrane Science, 2017, 537: 283–296
142. Lam C X F, Mo X M, Teoh S H, Hutmacher D W. Scaffold development using 3D printing with a starch-based polymer. Materials Science and Engineering C, 2002, 20(1–2): 49–56
143. Mandala R, Bannoth A P, Akella S, Rangari V K, Kodali D. A short review on fused deposition modeling 3D printing of bio-based polymer nanocomposites. Journal of Applied Polymer Science, 2022, 139(14): 51904
144. Moradi M, Meiabadi S, Kaplan A. 3D printed parts with honeycomb internal pattern by fused deposition modelling; experimental characterization and production optimization. Metals and Materials International, 2019, 25(5): 1312–1325
145. Sathies T, Senthil P, Anoop M S. A review on advancements in applications of fused deposition modelling process. Rapid Prototyping Journal, 2020, 26(4): 669–687
146. Tamir T S, Xiong G, Fang Q, Dong X. A feedback-based print quality improving strategy for FDM 3D printing: an optimal design approach. International Journal of Advanced Manufacturing Technology, 2021, 120: 2777–2791
147. Noraihan T, Tuan A, Abdullah A M, Akil H. Recent developments in fused deposition modeling-based 3D printing of polymers and their composites. Polymer Reviews, 2019, 59(4): 1–36
148. Plymill A, Minneci R, Greeley D A. Graphene and carbon nanotube PLA composite feedstock development for fused deposition modeling. Chancellor's Honors Program Projects. Knoxville: Univerity of Tennessee, 2016, 4–5
149. Ning F, Cong W, Hu Y, Wang H. Additive manufacturing of carbon fiber-reinforced plastic composites using fused deposition modeling: effects of process parameters on tensile properties. Journal of Composite Materials, 2017, 51(4): 451–462
150. Mazzanti V, Malagutti L, Mollica F. FDM 3D printing of polymers containing natural fillers: a review of their mechanical properties. Polymers, 2019, 11(7): 1094
151. Mohamed O A, Hasan S, Bhowmik J L. Studies on effect of fused deposition modelling process parameters on ultimate tensile strength and dimensional accuracy of nylon. IOP Conference Series: Materials Science and Engineering, 2016, 149(1): 012035
152. Wickramasinghe S, Do T, Tran P. FDM-based 3D printing of polymer and associated composite: a review on mechanical properties, defects, and treatments. Polymers, 2020, 12(7): 1529
153. Jayanth N, Senthil P, Prakash C. Effect of chemical treatment on tensile strength and surface roughness of 3D-printed ABS using the FDM process. Virtual and Physical Prototyping, 2018, 13(3): 155
154. Han T, Kundu S, Nag A, Xu Y. 3D printed sensors for biomedical applications: a review. Sensors, 2019, 19(7): 1706
155. Balogun H A, Sulaiman R, Marzouk S S, Giwa A, Hasan S W. 3D printing and surface imprinting technologies for water treatment: a review. Journal of Water Process Engineering, 2019, 31(2): 100786
156. Kumar A V. A review paper on 3D-printing and various processes used in the 3D-printing. Interantional Journal of Scientific Research in Engineering and Management, 2022, 6(5): 953–958
157. Puzatova A, Shakor P, Laghi V, Dmitrieva M. Large-scale 3D printing for construction application by means of robotic arm and gantry 3D printer: a review. Buildings, 2022, 12(11): 2023
158. Xiao J, Ji G, Zhang Y, Ma G, Mechtcherine V, Pan J, Wang L, Ding T, Duan Z, Du S. Large-scale 3D printing concrete technology: current status and future opportunities. Cement and Concrete Composites, 2021, 122: 104115
159. Zuo Z, De Corte W, Huang Y, Chen X, Zhang Y, Li J, Zhang L, Xiao J, Yuan Y, Zhang K, et al. Strategies towards large-scale 3D printing without size constraints. Virtual and Physical Prototyping, 2024, 19(1): e2346821
160. Low Z X, Chua Y T, Ray B M, Mattia D, Metcalfe I S, Patterson D A. Perspective on 3D printing of separation membranes and comparison to related unconventional fabrication techniques. Journal of Membrane Science, 2017, 523: 596–613
161. DePalma K, Walluk M R, Murtaugh A, Hilton J, McConky S,

Hilton B. Assessment of 3D printing using fused deposition modeling and selective laser sintering for a circular economy. Journal of Cleaner Production, 2020, 264: 121567

162. Siddique T H M, Sami I, Nisar M Z, Naeem M, Karim A, Usman M. Low cost 3D printing for rapid prototyping and its application. In: 2019 2nd International Conference on Latest Trends in Electrical Engineering and Computing Technologies. Islamabad: Institute of Electrical and Electronis Engineers, 2019, 1–5
163. Kazmer D, Peterson A M, Masato D, Colon A R, Krantz J. Strategic cost and sustainability analyses of injection molding and material extrusion additive manufacturing. Polymer Engineering and Science, 2023, 63(3): 943–958
164. Guillen G, Hoek E M V. Modeling the impacts of feed spacer geometry on reverse osmosis and nanofiltration processes. Chemical Engineering Journal, 2009, 149(1–3): 221–231
165. Li Y L, Tung K L. CFD simulation of fluid flow through spacer-filled membrane module: selecting suitable cell types for periodic boundary conditions. Desalination, 2008, 233(1–3): 351–358
166. Fimbres-Weihs G A, Wiley D E. Review of 3D CFD modeling of flow and mass transfer in narrow spacer-filled channels in membrane modules. Chemical Engineering and Processing, 2010, 49(7): 759–781
167. Bucs S S, Radu A I, Lavric V, Vrouwenvelder J S, Picioreanu C. Effect of different commercial feed spacers on biofouling of reverse osmosis membrane systems: a numerical study. Desalination, 2014, 343: 26–37
168. Salcedo-Díaz R, García-Algado P, García-Rodríguez M, Fernández-Sempere J, Ruiz-Beviá F. Visualization and modeling of the polarization layer in crossflow reverse osmosis in a slit-type channel. Journal of Membrane Science, 2014, 456: 21–30
169. Radu A I, Bergwerff L, van Loosdrecht M C M, Picioreanu C. A two-dimensional mechanistic model for scaling in spiral wound membrane systems. Chemical Engineering Journal, 2014, 241: 77–91
170. Foo K, Liang Y Y, Weihs G A F. CFD study of the effect of SWM feed spacer geometry on mass transfer enhancement driven by forced transient slip velocity. Journal of Membrane Science, 2020, 597: 117643
171. Chong Y K, Liang Y Y, Weihs G A F. Validation and characterisation of mass transfer of 3D-CFD model for twisted feed spacer. Desalination, 2023, 554: 116516
172. Chong Y K, Liang Y Y, Lau W J, Fimbres Weihs G A. 3D CFD study of hydrodynamics and mass transfer phenomena for spiral wound membrane submerged-type feed spacer with different node geometries and sizes. International Journal of Heat and Mass Transfer, 2022, 191: 122819
173. Okereke M, Keates S. In: finite element applications. Springer Tracts in Mechanical Engineering. Cham: Springer, 2018, 243–297
174. Lou J, Johnston J, Cath T Y, Martinand D, Tilton N. Computational fluid dynamics simulations of unsteady mixing in spacer-filled direct contact membrane distillation channels. Journal of Membrane Science, 2021, 622: 118931
175. Gu B, Adjiman C S, Xu X Y. Correlations for concentration polarization and pressure drop in spacer-filled RO membrane modules based on CFD simulations. Membranes, 2021, 11(5): 338
176. Lipnizki F, Lipnizki J, Hjertager B H, Hansen R, Hvidberg J, Solberg T, Ibsen C H, Jonsson G. Membrane spacers for ultrafiltration: modelling of mass transfer and pressure. In: IMSTEC '03 - The 5th Int Membrane Science and Technology Conference. Sydney: University of New South Wales, 2003
177. El Kadi K, Janajreh I, Hashaikeh R. Numerical simulation and evaluation of spacer-filled direct contact membrane distillation module. Applied Water Science, 2020, 10(7): 174
178. Ahmad A L, Lau K K. Impact of different spacer filaments geometries on 2D unsteady hydrodynamics and concentration polarization in spiral wound membrane channel. Journal of Membrane Science, 2006, 286(1–2): 77–92
179. Subramani A, Kim S, Hoek E M V. Pressure, flow, and concentration profiles in open and spacer-filled membrane channels. Journal of Membrane Science, 2006, 277(1–2): 7–17
180. Picioreanu C, Vrouwenvelder J S, van Loosdrecht M C M. Three-dimensional modeling of biofouling and fluid dynamics in feed spacer channels of membrane devices. Journal of Membrane Science, 2009, 345(1–2): 340–354
181. Kavianipour O, Ingram G D, Vuthaluru H B. Investigation into the effectiveness of feed spacer configurations for reverse osmosis membrane modules using computational fluid dynamics. Journal of Membrane Science, 2017, 526: 156–171